SAPIENZA
Università di Roma
Facoltà di Scienze Matematiche Fisiche e Naturali

DOTTORATO DI RICERCA
IN BIOLOGIA CELLULARE E DELLO SVILUPPO

XXXII Ciclo
(A.A. 2019/2020)

Characterization of patients with mitochondrial disease: assessment of the pathological phenotype associated with genes involved in mitochondrial quality control and dynamics.

Dottoranda

Giulia Trani

Docente guida

Dr.ssa Rosalba Carrozzo

Tutore

Prof.ssa Silvia Francisci
Prof.ssa Daniela Uccelletti

Coordinatore

Prof. Giulia De Lorenzo

Index

General introduction

Mitochondria are subcellular organelles found in all eukaryotic cells, except in red blood cells; they are implicated in multiple cellular processes and consist of two membranes, the inner mitochondrial membrane (IMM) and the outer mitochondrial membrane (OMM), and of two aqueous compartments, the matrix and the intermembrane space. The IMM area is several-fold larger than the one of OMM, due to the fact that in the IMM there are some invaginations called *cristae* which contain the electron transport chain complexes from I to IV (complex I, CI; complex II, CII; complex III, CIII; complex IV, CIV) and the F1-F0-ATP synthase (CV). This multicomplex system is responsible for energy production, in the form of adenosine 5′-triphosphate (ATP), via the oxidative phosphorylation (OXPHOS). The transport of electrons, provided by carrier molecules such as NADH or $FADH_2$, through the four complexes of the respiratory chain, with the help of two mobile electron shuttles (coenzyme Q and cyt *c*), generates energy, used by CI, CIII and CIV to pump protons across the IMM thus creating an electrochemical potential ($\Delta\Psi$). This electrochemical potential is the driving motor of the complex V and lead to the production of ATP, but is also responsible for the thermogenesis, the import of Ca^{2+} and the translocation of proteins inside the mitochondria (Ghezzi and Zeviani, 2018).

Mitochondria contain a small circular multicopy genome (16569 base pair) (mitochondrial DNA (mtDNA)) that is maternally inherited and contains only 37 genes encoding for 22tRNA, 2 rRNA and 13 proteins, which take part in the respiratory chain complexes, with the exception of CII. Based on the fact that each complex is composed by numerous additional subunits nuclearly-encoded, the assembly of each OXPHOS complex requires the insertion into IMM of both mtDNA- and nuclear DNA (nDNA) encoded subunits. Thus, the genetic basis of the OXPHOS is unique, with the involvement of both nuclear and mitochondrial DNA.

In addition to energy production, mitochondria are involved in many biological functions, including the regulation of reactive oxygen species (ROS), biogenesis of the Fe-Cu clusters, heme synthesis, metabolism of amino acids and lipids, apoptosis and mitophagy (Gorman *et al*. 2016). Given their fundamental role in the physiology of the whole cell, mitochondria undergo to a tightly regulation, since any of their dysfunction can lead to dramatic consequences.

Mitochondrial diseases (MDs) are a group of very heterogeneous and rare genetic disorders that affect mitochondrial respiratory chain function and cellular energy production. MDs can arise from both nuclear or mtDNA mutations, can occur at

any age and, although the most affected tissues are those with high energy demand such as brain, muscle and heart, the clinical signs could involve also liver, heart, kidney, eye and ear (Suomalainen and Battersby, 2018). The incidence of MDs is 1:5000 live birth (Gorman *et al*., 2016; Craven *et al*., 2017) considering only the mutation that affect the mtDNA and even higher by including some frequent nuclear gene mutations, reaching the incidence of 1:2000 individuals (Suomalainen and Battersby, 2018).

In the last years, the breakthrough of next-generation sequencing (NGS) approaches for genetic diagnosis has expanded the genetic heterogeneity of MDs (Stenton and Prokisch, 2018). More than 1,500 genes that are encoded in the nucleus, synthesize proteins targeted to mitochondria. Mutations can lead to mitochondrial dysfunction by different modes of transmission: sporadic, maternal, autosomal recessive, autosomal dominant or X-linked. Thus, mitochondrial diseases can follow any inheritance model, and are probably one of the most heterogeneous conditions known in the whole field of human genetic disorders.

The maintenance of "healthy" and fully functional mitochondria is essential for cellular homeostasis. In this regard, the cell has evolved various mechanisms dedicated to the maintenance of the mitochondrial proteome such as mitochondrial dynamics and mitochondrial quality control. A first check point and active surveillance is provided by the organelle itself. The mitochondria have their own chaperones and proteolytic enzymes that remove damaged or unfolded proteins (Matsushima and Kaguni, 2012). The plasticity of the mitochondria allows continuous changes of their shape and number, while their morphology is maintained by the equilibrium of fusion and fission event.

Mitochondria undergo fusion and fission in order to avoid damage accumulation or respond to certain bioenergetics demands (Campello and Scorrano, 2010). In recent years, a significant number of mutations in genes involved in mitochondrial dynamics and mitochondrial quality control have been recognized as the genetic cause of MDs.

In our laboratory through the use of NGS technology we identify new mutations in genes involved in mitochondrial dynamics and in mitochondria quality control and we have functionally characterized these mutations and demonstrated their pathogenic roles in the analyzed patients.

Aims of the work

The new mutations identified using the NGS technology expand the number of mutations on genes involved in mitochondrial dynamics and in mitochondria quality control.

The main aim of my thesis is to characterize such mutations, proving their pathogenicity and demonstrate a genotype-phenotype correlation. The use of patients' primary fibroblast as a cellular model has been a useful tool to verify the involvement of the mutated protein in specific pathways such as mitochondrial dynamics and mitochondrial quality control. In addition to histochemical and biochemical study, *in vivo* and *in silico* models have been applied.

A basic understanding of the molecular mechanism involved in these mitochondrial pathways also can offer, in future, the opportunity to identify potential therapeutic targets in order to assess whether the use of new molecules could enable the recovery of the mitochondrial homeostasis and, therefore, the recovery of the phenotype as well.

Summary

The maintenance of healthy and functional mitochondria is essential for cellular homeostasis; a first check point is provided by the organelle itself through the mitochondrial quality control and through the mitochondrial dynamics**.** One of the main players of the mitochondrial quality control is the Lon protease encoded by *LONP1* gene, involved in mitochondrial proteostasis and in the maintenance of mitochondrial DNA. Mutations in *LONP1* were associated with a multisystem disorder called CODAS (Cerebral, Ocular, Dental, Auricular, Skeletal) syndrome (Strauss *et al*. 2015) and, more recently, with a classical mitochondrial disease phenotype (Peter *et al.* 2018; Nimmo *et al*. 2019). Furthermore, mitochondrial dynamics involve the Drp1 protein, a large dynamin-like GTPases encoded by *DNM1L* gene, that is responsible for fission of mitochondria. Mutations in *DNM1L* gene have been associated with several neurological disorders (Schmid *et al*. 2019).

Through the use of Next Generation Sequencing (NGS) technology, we identified new mutations in genes involved in mitochondrial quality control and dynamics. In one patient, we found three different mutations in *LONP1*, never described. These variants cause both energy defects and alterations in mitochondrial network. In five patients, we identified *de novo* dominant *DNM1L* variants, two of which have been never reported. Also in these cases, patients' fibroblast displayed defects in mitochondrial morphology; interestingly, we observed, in muscle biopsies, changes in mitochondrial distribution. To date no peculiar histochemical alterations have been reported in *DNM1L*-mutated patients and this can represent a diagnostic tool.

Sommario

Il mantenimento dell'omeostasi cellulare è strettamente dipendente dai mitocondri, la cui funzionalità è innanzitutto regolata dall'organello stesso attraverso il controllo di qualità e il corretto *network* mitocondriale. Uno dei maggiori responsabili del controllo di qualità mitocondriale è la proteasi Lon codificata dal gene *LONP1*, coinvolta nella proteostasi e nel mantenimento del DNA mitocondriale. Mutazioni in questo gene sono state associate ad un disordine multisistemico noto come sindrome CODAS (Strauss *et al*. 2015). Recentemente, mutazioni in *LONP1* sono state riconosciute come la causa di condizioni patologiche con caratteristiche cliniche associabili alle malattie mitocondriali (Peter *et al*. 2018; Nimmo *et al*. 2019). Nei processi della dinamica mitocondriale un ruolo fondamentale è svolto dalla dinamina Drp1, responsabile

della fissione mitocondriale e codificata dal gene *DNM1L*. Mutazioni in questo gene sono state associate a diversi disordini neurologici (Fahrner *et al*. 2016).
L'utilizzo di tecnologie di nuova generazione (NGS) ci ha permesso di identificare nuove mutazioni in geni coinvolti nel controllo di qualità e nella dinamica mitocondriali. In un paziente abbiamo riscontrato tre diverse mutazioni in *LONP1*, mai finora descritte. Le varianti identificate determinano sia difetti energetici che alterazioni del *network* mitocondriale. In altri cinque pazienti, abbiamo invece individuato varianti *de novo* nel gene *DNM1L*, due delle quali non sono mai state riportate. Anche in questo caso nei fibroblasti dei pazienti abbiamo osservato difetti della morfologia mitocondriale, mentre nel tessuto muscolare abbiamo riscontrato alterazioni della distribuzione dei mitocondri a livello delle fibre muscolari. È importante sottolineare che tali alterazioni istopatologiche non erano mai state osservate in precedenza e possono rappresentare un tratto diagnostico per la ricerca di mutazioni nel gene *DNM1L*.

I PART

Introduction

Mitochondrial fission and fusion are essential mechanisms, known as mitochondrial dynamics, involved in the regulation of the cellular homeostasis. Once mitochondria were considered "static bean-shaped" organelles, but now it is well established that mitochondria assemble into a network that is very dynamic and undergoes dimensional and structural changes to meet specifics energy needs of the cell. Since mitochondria are dynamic organelles, capable of fusion, fragmentation, biogenesis, mitophagy, and intra- or inter- cellular transport, the overall state of the mitochondrial network and its distribution within a cell are fluid (Valente et al, 2019).

Mitochondrial dynamics are driven by a set of dynamin's family members, the large guanosines triphosphate hydrolases (GTPases) that are well conserved between yeast, flies, and mammals. Fission is mediated by a cytosolic dynamin family member called Drp1, encoded by *DNM1L* gene. When activated DRP1 is recruited by the mitochondrial dynamics' proteins 49 and 51 kDa (MiD49 and MiD51), and the mitochondrial fission factor (Mff) to the outer mitochondrial membrane, where it binds its receptor, the mitochondrial fission protein 1 (Fis1) and multimerizes, creating a ring-like structure that constricts and divides the organelle. Moreover, Drp1 is also involved in the perossisomal fission, acting with a similar mechanism division (Schrader et al., 2016). Opposed to fission, fusion between mitochondrial fusion between mitochondrial inner membranes is mediated by a single dynamin family member called Opa1, whereas fusion of the outer membranes is mediated by membrane-anchored dynamin family members named mitofusins (Mfn1 and Mfn2) (Youle *et al*. 2012).

Mitochondrial fission and fusion machineries are regulated by proteolysis and post-translational modifications. In particular the regulation of DRP1 by post-translational modifications is important for DRP1 translocation to mitochondria. Phosphorylation of DRP1 at Ser 616 (S616) by cyclin dependent kinase (CDK) 1/Cyclin B or CDK5 promotes mitochondrial fission during mitosis. In contrast, DRP1-S637 phosphorylation by protein kinase A (PKA) induces the detachment of DRP1 from mitochondria and inhibits mitochondrial fission (Pagliuso, Cossart and Stavru, 2018). It is demonstrated that mitochondrial fission is essential for growing and dividing cells to populate them with adequate numbers of mitochondria and to ensure the presence of mitochondria at sites of high ATP consumption. Knockout studies in mice showed that deletion of Drp1 is embryonically lethal, indicating that mitochondrial fission is an essential process

(Ishihara *et al.*, 2009). At a cellular level, mitochondrial fission is important for organelle distribution during mitosis (Horbay and Bilyy, 2016) and for proper distribution of mitochondria to neuronal synapses, where localized energy production supports synaptic functions (Wakabayashi *et al.*, 2009).
A fine regulation between fission and fusion is needed to a proper mitochondrial function and alterations in genes involved in the process of mitochondrial dynamics is related to many human diseases. Up to date mutations have been found in the following genes:

- *MFN2* (OMIM#609260), associated with the peripheral neuropathy Charcot–Marie–tooth disease type 2a (Stuppia *et al*., 2015);
- *OPA1* (OMIM#165500), that lead to the autosomal dominant optic atrophy (ADOA), a pathological condition characterized by the loss of some or most of the fibres of the optic nerve (Lenaers *et al*., 2012);
- *OPA3* (OMIM#258501), associated Optic Atrophy and increased excretion of 3-methylglutaconic acid (Ankister *et al*. 2001);
- *GDAP1* (OMIM#607831), mutations in this gene cause the Charcot–Marie–Tooth 2K (Chung*et a*l. 2008);
- *MIEF2* associated with mitochondrial myopathy (Bartsakoulia et al., 2018).

DRP1 impairment, associated with either *de novo* dominant or compound heterozygous mutations (MIM #603850), is implicated in several neurological disorders characterized by early onset encephalopathy, psychomotor delay, hypotonia, progressive course and death in childhood. Many patients develop refractory seizures, consistent with an epileptic encephalopathy, and thereafter show neurological decline. Cultured fibroblasts from patients with these genetic conditions usually show abnormally elongated mitochondria and aberrant peroxisomes (Fahrner *et al.*, 2016; Nasca et al., 2016).
In this thesis, I describe five patients affected by severe epileptic encephalopathy associated with *de novo* dominant mutations in *DMN1L*, three of which never reported before. Cultured fibroblasts displayed the classical altered mitochondrial and peroxisomal network; moreover, mitochondrial alterations have been observed in the muscle biopsy. The muscle's peculiarity has been for the first time associated with mutations in *DNM1L*.

Results

Case reports

The patients described here are affected by early onset encephalopathy with microcephaly and drug resistant seizures, progressive brain atrophy or abnormal brain development, and occasionally persistent lactic acidemia.

Mutational analysis

Bioinformatics analysis carried out on the TruSight One panel (for Pt.1, Pt.2 and Pt.3) and on a targeted mitochondrial panel (for Pt.4 and Pt.5) led to the identification of a single gene entry, *DNM1L* (NM_012062, NP_036192). Six different mutations have been detected in DNM1L (NM_012062), all resulted absent in public (dpSNP142, ExAC, 1000 Genomes, HGMD, gnomAD) and in-house databases. The identified variants are reported in **Table 1**.

Patient	Mutation	Aminoacid change	Segregation	References
Pt.1	c.668G>T	p.Gly.223Val	*de novo*	-
Pt.2	c.1207C>T	p.Arg403Cys	*de novo*	Fahrner *et al.*, 2016; Schmid *et al.*, 2019
Pt.3	c.1109T>G	p.Phe370Cys	*de novo*	-
Pt.4*	c.1085G>A c.1535T>C	p.Gly362Asp p.Ile512Thr	*de novo* (?) mother	- Vanstone *et al.*, 2016
Pt.5	c.1084G>A	p.Gly362Ser	*de novo*	Sheffer *et al.*, 2015

Table 1: The variants have been identified by NGS and confirmed by Sanger sequencing in all patients and their parents. In Pt.4 the first variant c.1085 G>A is a *de novo* event and the second variant c.1535 T>C was inherited from the mother. SIFT (http://sift.jcvi.org) and PolyPhen-2 (http://genetics.bwh.harvard.edu/pph2) were used for pathogenicity prediction of the variants**.**

Segregation in the families was negative for all mutations (**Figure 1A-E**), and this speak for a *de novo* event, except for the p.Ile512Thr identify in Pt.4 which was inherited from the mother (**Figure 1D'**). An in-depth evaluation of the familiar history of Pt.4 revealed that the mother had a son with epileptic encephalopathy from another man. This child died at 3 years of age and no material was available for genetic studies. By subcloning PCR products obtained from Pt.4's cDNA, we were able to assess that the two *DNM1L* variants were on the same allele (i.e., the maternal allele). Moreover, a further analysis of *DNM1L* genomic region using a next- generation sequencing (NGS) approach revealed that the c.1085G>A was present in the mother's blood DNA, although at very low level (~5%) (**Figure 2 A-B**). These findings suggested a maternal germline mosaicism for the dominant mutation c.1085G>A (p.Gly362Asp), that may even explain the affected status of the Pt.4's half-brother.

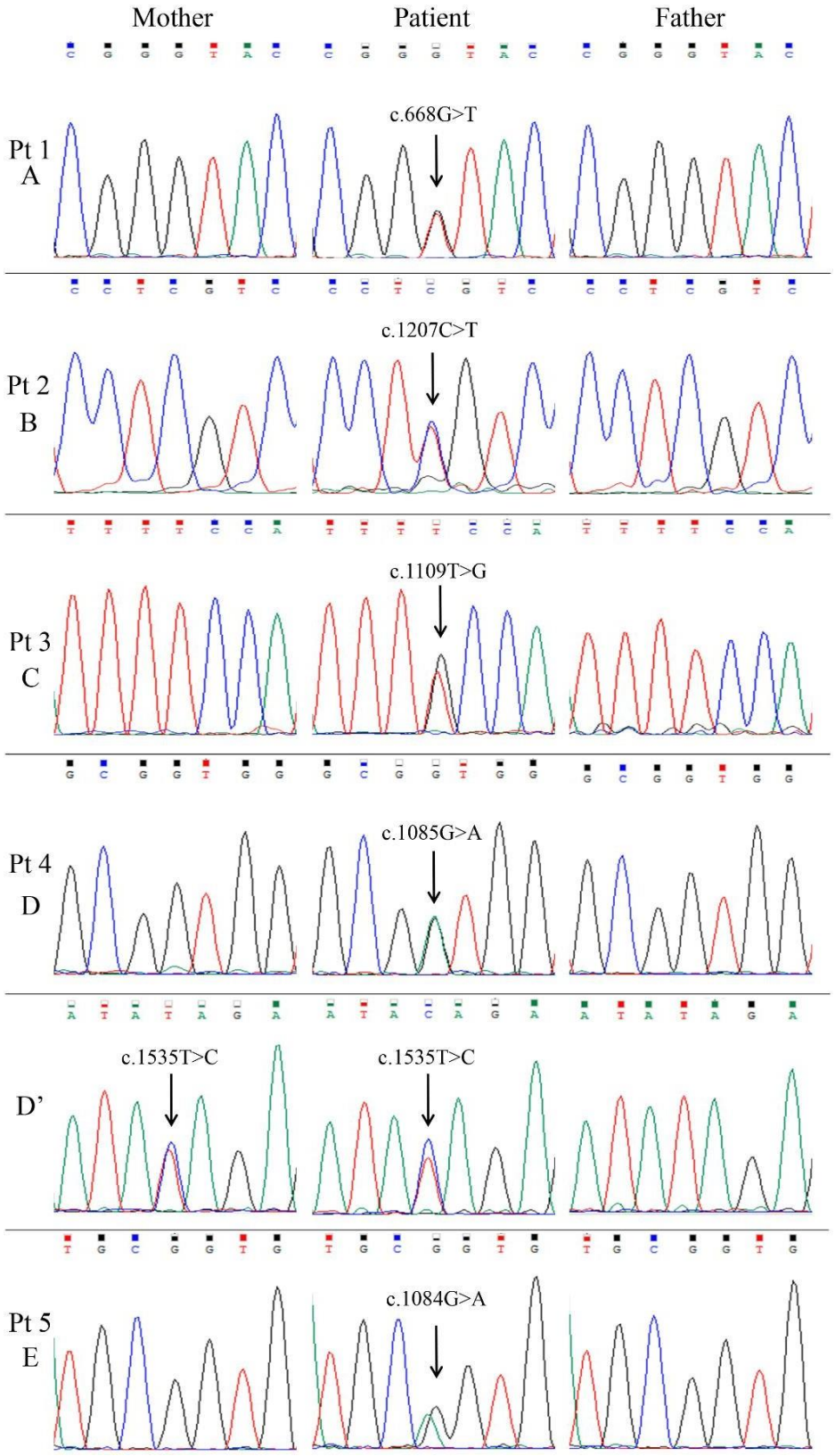

Figure 1 Electropherograms. The variants identified by NGS in *DNM1L* (**A-E**) have been confirmed by Sanger sequencing in all patients and their parents. In **D'** the second variant identified in Pt.4 (c.1535T>C) was inherited from the mother.

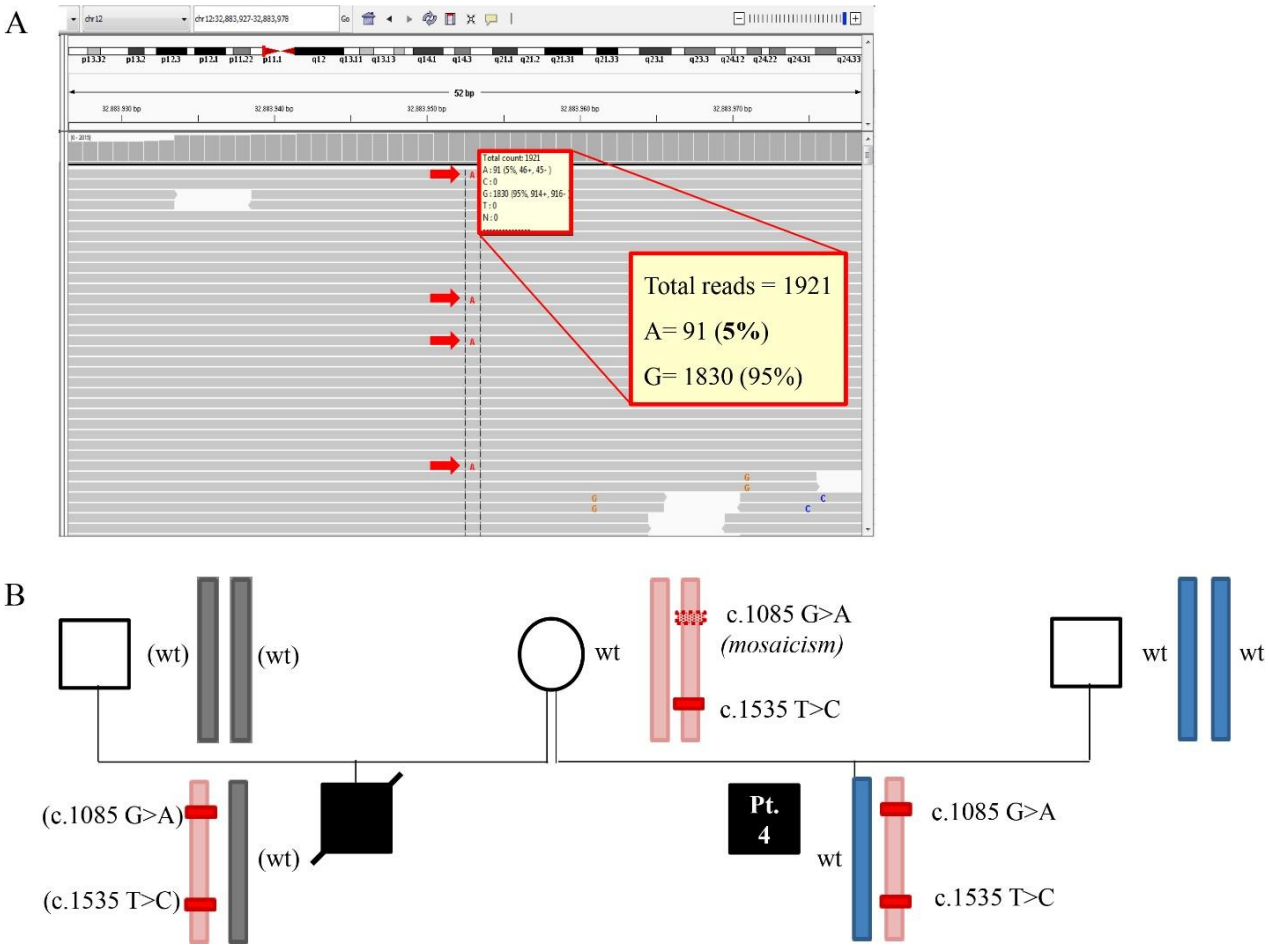

Figure 2: **Segregation analysis in the family of Pt.4**. (A) NGS analysis revealed 5% c.1085G>A variant in blood DNA from Pt.4's mother, indicating germinal mosaicism. (B) Pedigree and reconstruction of the DNM1L alleles in Pt.4's family members. Genotypes under brackets are hypothesized but not tested because DNA was not available.

Histological and biochemical analyses

Histochemistry of the muscle sample of Pt.1, Pt.2, Pt.3 showed scattered fibers with a patchy reduction of cytochrome *c* oxidase (COX) and succinate dehydrogenase (SDH) stain with aspects of polymorphic core like areas (**Figure 3, left and central panels**). Similarly, areas of reduced immunoreactivity were observed using the TOMM20 antibody confirming impairment of the mitochondrial network distribution (Figure 3, right panel). Moreover, histochemical serial sections of the muscle biopsy in Pt. 3 showed that the fibers devoid of mitochondria were type 1 fibers (**Figure 4**). In Pt.4 histochemical examination of muscle tissue's mitochondria using electron microscopy revealed abnormal mitochondria that couple each other (**Figure 5**). OXPHOS biochemical analysis in muscle homogenate was normal in Pt.1, Pt.2, Pt.3 and Pt.4 (data not shown). Histochemistry of the muscle sample of a patient affected by an autosomal recessive mutation in *OPA1* (Nasca et al., 2017) was studied and compared with those of *DNM1L* patients and showed no patchy staining abnormalities (**Figure 3 lowest panel**).

In addition, by Long Range PCR we also searched comparatively for multiple deletions in muscle samples and found multiple deletions only in the *OPA1* mutated patient and no in the *DNM1L* patients (data not shown).

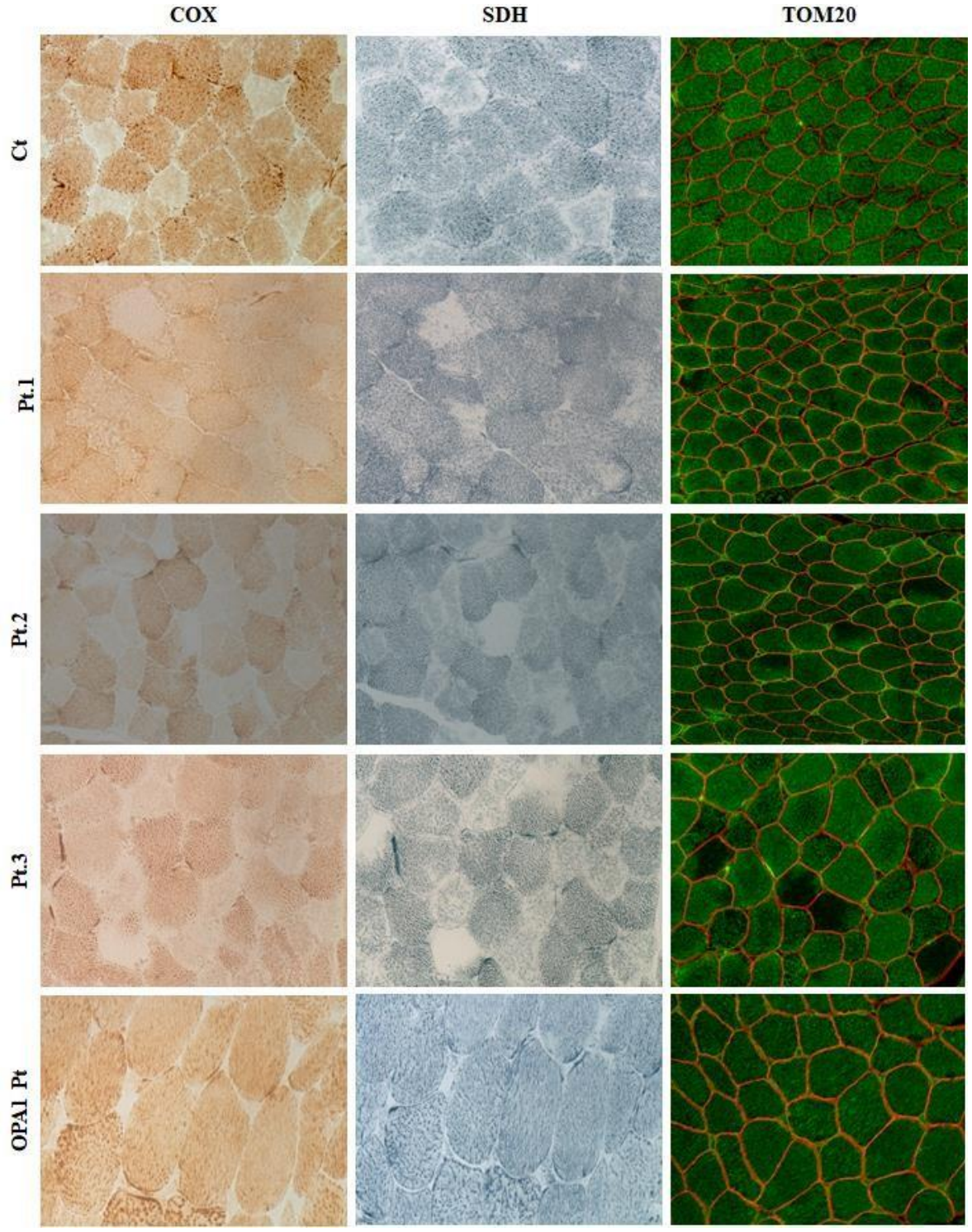

Figure 3: Panel showing the histochemistry of quadriceps muscle samples of Pt.1, Pt.2, Pt.3 and control. The muscle histochemistry of serial sections of three patients with heterozygous dominant mutations in DNM1L and stained with cytochrome c oxidase (COX) and succinate dehydrogenase (SDH) showed scattered fibers with a patchy reduction of both COX and corresponding SDH, with aspects of polymorphic core like areas (left and central panel). Similarly areas of reduced immunoreactivity was observed using the TOMM20 antibody confirming impairment of the mitochondrial network distribution (right panel). These abnormalities were not detected in the muscle biopsy of a patient with biallelic mutations in OPA1 (last bottom row) already described (Nasca *et al.,* 2017).

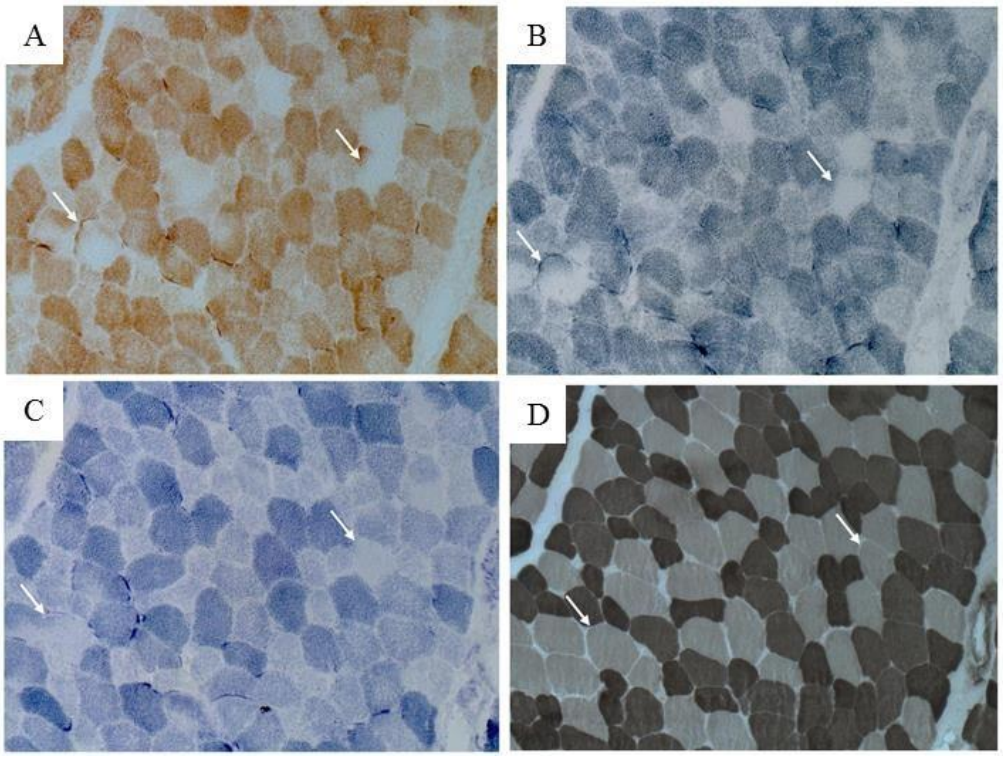

Fig.4: Histochemistry of the muscle biopsy of Pt.3 showing that serial fibers stained for COX (A), SDH (B), NADH (C) and ATPase 9.4 (D) that are devoid of mitochondria (arrows) are all type 1 fibers.

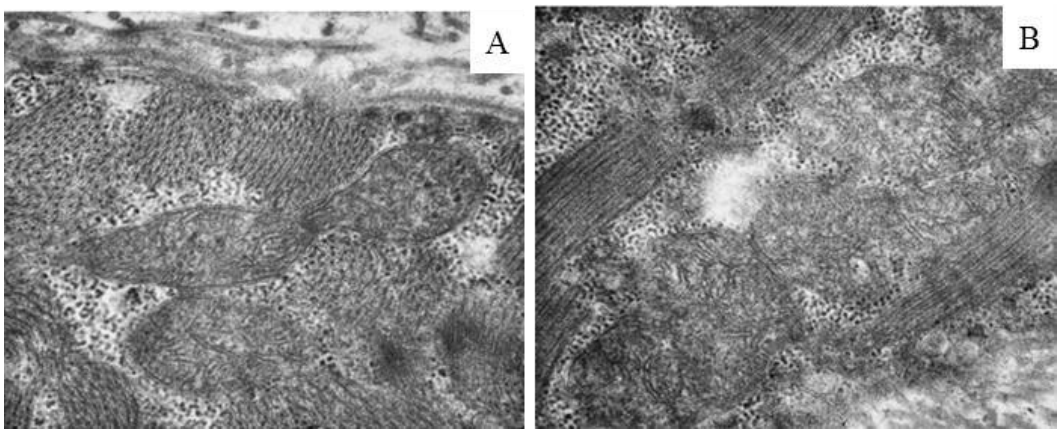

Fig.5: Histopathological aspects of the muscle biopsy of Pt.4. Electron microscopy shows enlarged mitochondria, which sometimes appear connected to each other. Original magnification 30000X.

Western blotting analysis

To evaluate the impact of the mutations on DRP1 stability, we performed WB analysis on fibroblasts. We observed a significantly increased (in Pt.3) or normal (in Pt.1, Pt.2, Pt.4 and Pt.5) level of the protein when normalized to GAPDH (**Figure 6A-B**), in contrast with the strong reduction present in *DNM1L*-recessive cases (Nasca et al., 2016). The expression level of OPA1 and of different subunits of the OXPHOS showed no differences compared to controls (data not shown).

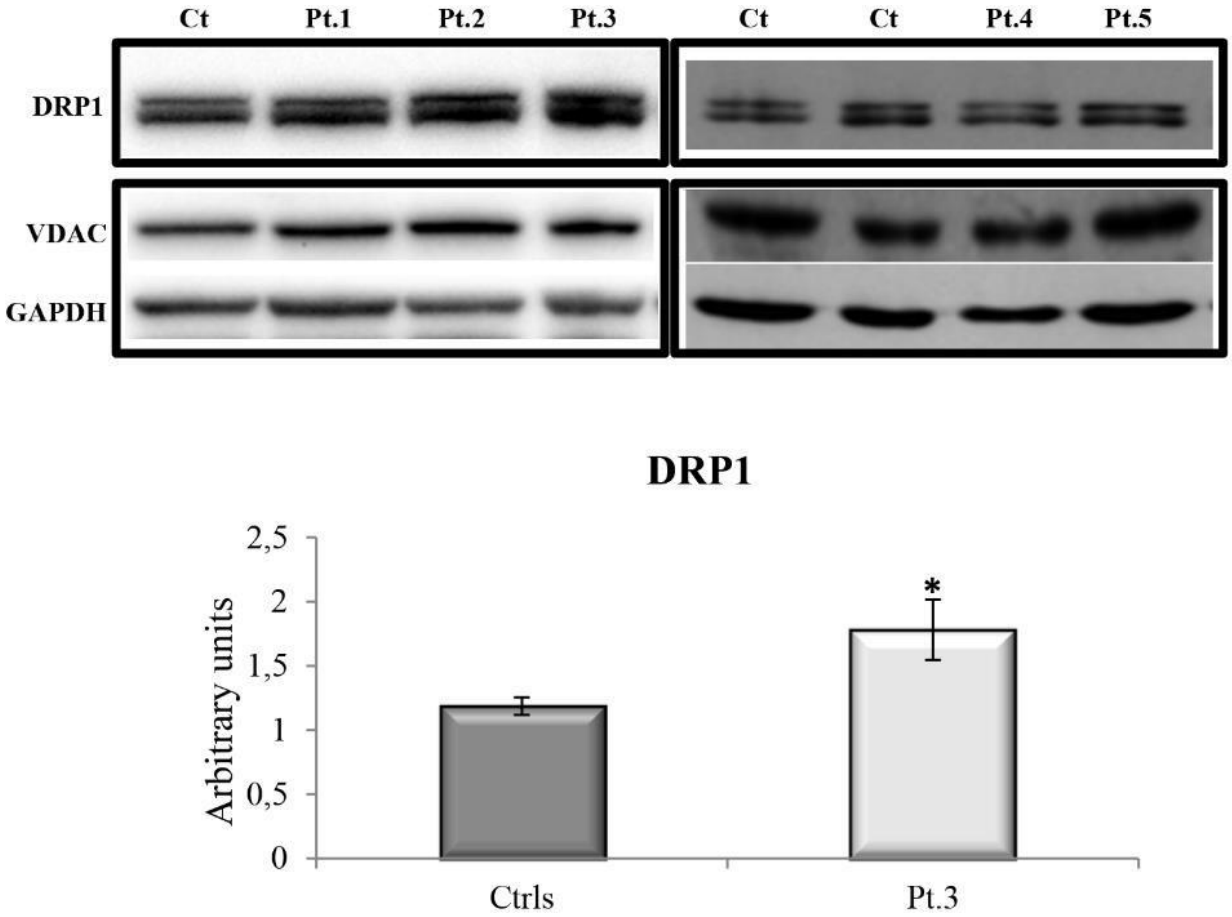

Figure 6 Western blotting analysis. Immunoblot analysis of total lysates from control subjects (Ct) and patient's (Pt) fibroblasts using α-DRP1, α-VDAC, and α-GAPDH antibodies. The latter was used as loading control. The state level of DRP1 protein is significantly increased in Pt.3 fibroblasts. Values in the graph are given as the mean ± SD (n = 4 to 5); *, p<0,05.

Tissue culture, Immunostaining and Imaging

Because of the pivotal role of DRP1 on dynamics of mitochondria and peroxisomes, we performed morphological studies on patients' fibroblasts. In normal glucose medium Pt.1 displayed a mixed population in which hyperfused mitochondria are associated with swollen and rod-shaped mitochondria and Pt.5 showed dot-shaped mitochondria (**Figure 7A-B, left panel**). In galactose-supplemented medium the mitochondrial network of *DNM1L*-mutant fibroblasts showed a lower tendency to fuse associated with a more disorganized network with swollen, dots, rings, and "chain-like" structures (**Figure 7A-B, right panels**). For the immuno- staining of peroxisomes, we used an antibody against PMP70 and organelles appear longer, larger, and less uniformly distributed into cytoplasm in Pt.4 and Pt.5 in contrast with the highly diffused punctuated staining present in control cells (**Figure 7C**).

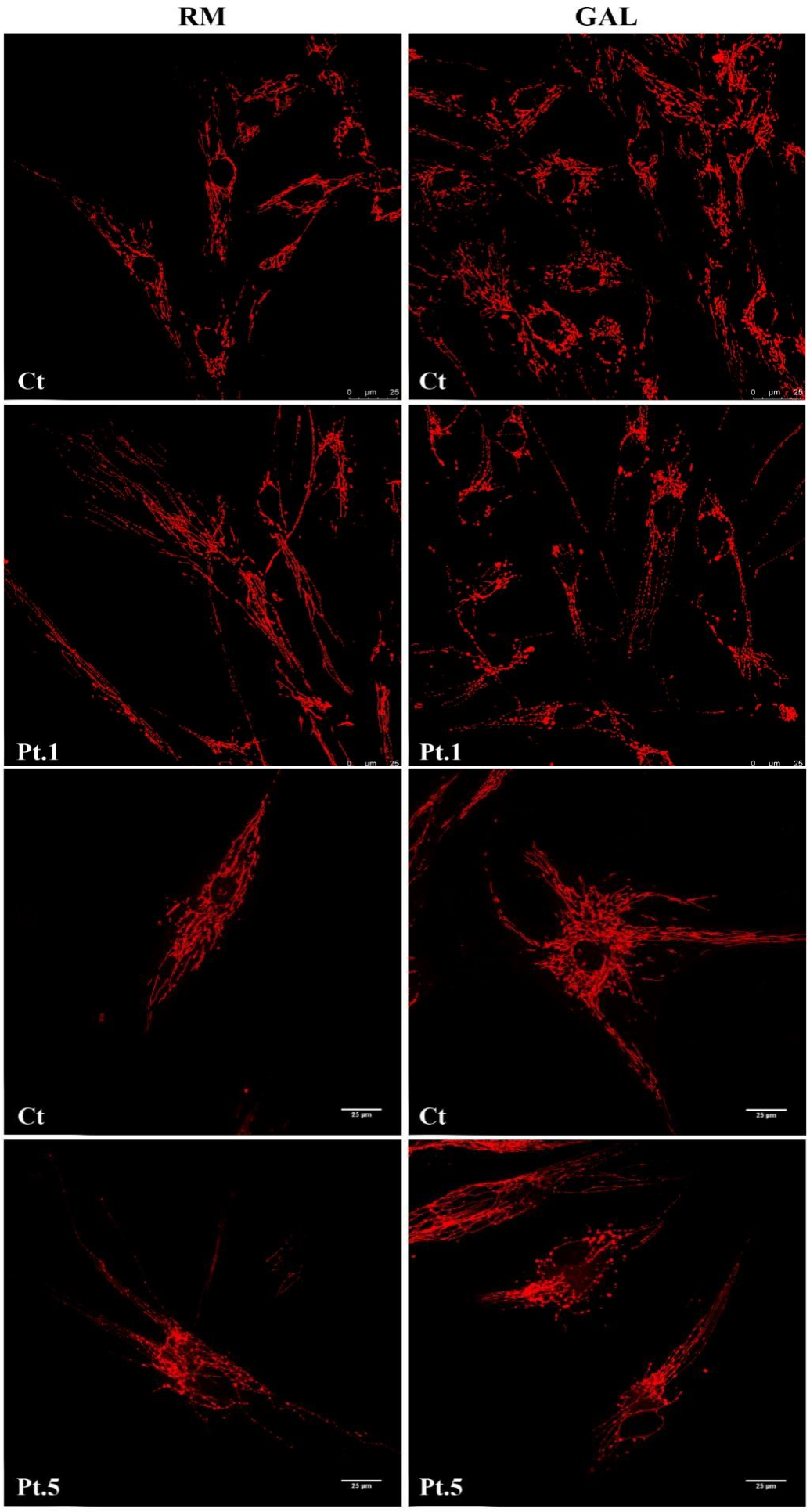
RM
GAL
A
Ct
Ct
Pt.1
Pt.1
B
Ct
Ct
Pt.5
Pt.5

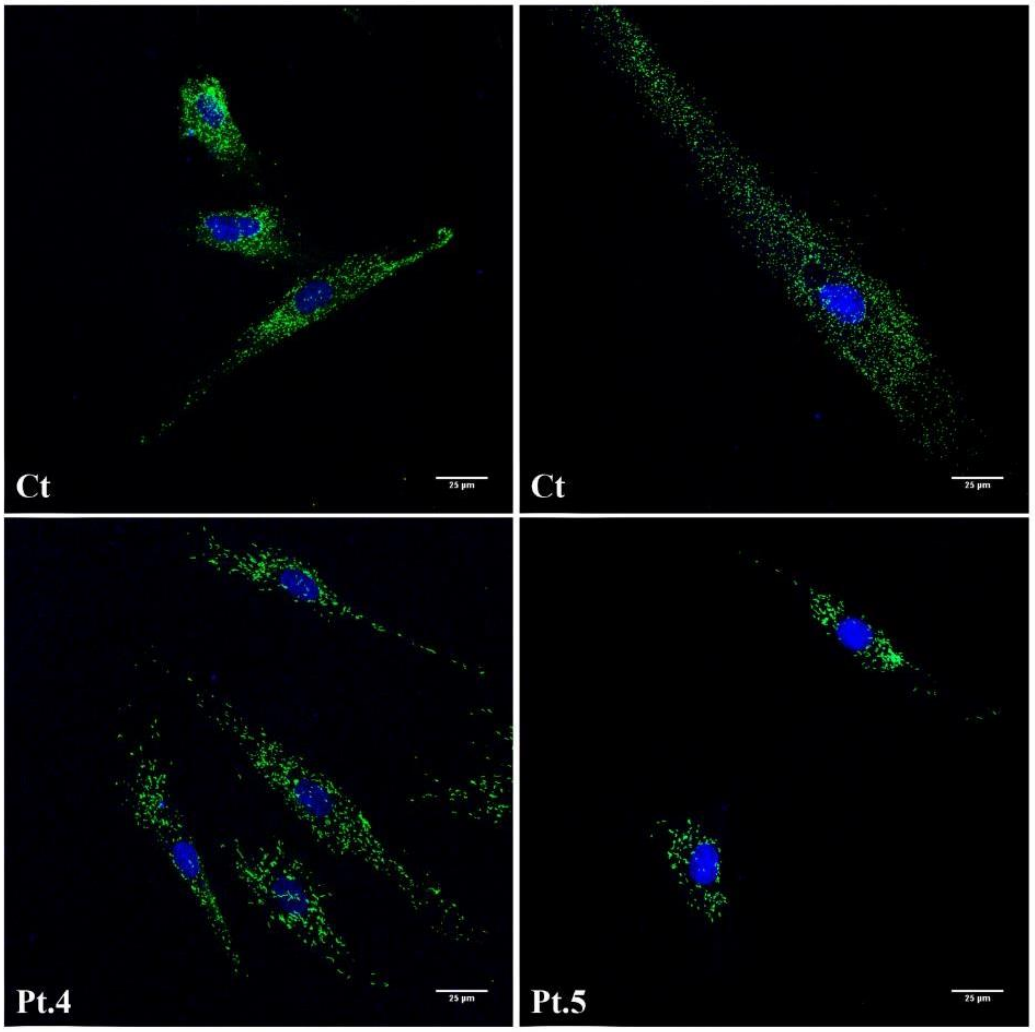

Figure 7: Characterization of the mitochondrial and peroxisomal network: analysis by fluorescence microscopy. (A-B): We used the antibody TOMM20 in fixed cells for Pt.1 or Mitotracker red in living cells for Pt.5, both specific for mitochondrial staining. (C): Immunofluorescence staining with the anti-PMP70 antibody of fibroblasts from Ct, Pt.4 and Pt.5 (Scale bar: 25 µm).

Functional studies in yeast

The deleterious effect of the p.Arg403Cys substitution was already experimentally demonstrated (Fahrner et al. 2016). To assess the pathogenic role of the other identified *DNM1L* variants as well as to compare the effects of different substitutions on the same amino acid (p.Gly362), we performed complementation studies in a *S. cerevisiae* strain lacking *DNM1*, hereafter referred to as *Δdnm1*. *DNM1* is the yeast orthologue of human *DNM1L;* the amino acid residues corresponding to p.Gly223Val, p.Gly362Asp, p.Gly362Ser and p.Ile512Thr variants are conserved between the two species, being in yeast p.Gly252, p.Gly397, p.Ile543, whereas human p.Phe370 is not conserved, being p.Tyr405 in yeast. The *dnm1*Δ strain was transformed either with the wt *DNM1*, the $dnm1^{G252V}$, $dnm1^{G397D}$, $dnm1^{G397S}$or $dnm1^{I543T}$ mutant alleles, under the endogenous *DNM1* promoter, as well as with the empty plasmid. To test the possible effects on mitochondrial function, we first evaluated the oxidative growth by spot assay analysis on medium supplemented with either glucose or ethanol or glycerol. The oxidative growth of the $dnm1^{G397D}$ and the $dnm1^{G397S}$ mutant strains was partially affected compared to the *DNM1* wild type strain whereas the growth of the $dnm1^{G252V}$ was similar to the strain *dnm1Δ*; on the contrary the growth of the $dnmI^{I543T}$ mutant was unaffected (**Figure 8A**). To further investigate the OXPHOS defect, the oxygen consumption was measured and according to the growth phenotype, the oxygen consumption rate of the $dnm1^{G397D}$ and of the $dnm1^{G397S}$ mutants was respectively 30% and 20% lower than that of the wild type strain, whereas the oxygen consumption rate of $dnm1^{G252V}$ and of the *dnm1* null strain was decreased by 60%; also, the $dnmI^{I543T}$ mutant showed a slight though significant reduction of respiratory activity (Figure 6B). Altogether these results validated the pathogenicity of the mutations Gly252Val, Gly397Asp and Gly397Ser, showing also that substitution of Gly397 with aspartate is more deleterious than substitution with serine. The amino acid change Ile543Thr slightly affects the activity of the protein too, being the respiratory activity altered compared to *DNM1* wild type. Since the variant Ile512Thr was present in the patient in *cis* with the Gly362Asp, we also constructed a yeast mutant allele carrying both the corresponding variants. Interestingly, the $dnm1^{G397D\text{-}I543T}$ strain showed a more severe phenotype than the strain carrying only the mutation Gly397Asp; in fact, the oxidative growth and the respiratory activity become similar to that of the null mutant suggesting that Ile543Thr is a phenotypic modifier (**Figure 8A-C**).

Finally, we tested whether the mutations have a dominant or recessive effect using a diploid hemizygous *DNM1*/*dnm1Δ* strain transformed with the plasmid having mutant alleles or with the empty vector and measuring the oxygen consumption. The respiratory activity of the heteroallelic strains *DNM1*/*dnm1*^{G397D}, *DNM1*/*dnm1*^{G397S} and *DNM1*/*dnm1*$^{G397D\text{-}I543T}$, but not that of *DNM1*/*dnm1*^{G252V} and *DNM1*/*dnm1*^{I543T}, was lower compared to the hemizygous strain *DNM1*/*dnm1Δ*. This indicates that Gly397Asp and Gly397Ser have a partial dominant-negative effect whereas Ile543Thr and, quite unexpectedly, Gly252Val act as recessive mutations (**Figure 8C**), at best concerning the effect on oxygen consumption. To better deepen this point, we investigated in the heteroallelic strain *DNM1*/*dnm1*^{G252V} another phenotype, i.e the *petite* frequency, based on the observation that the mutation Lys41Ala, generally recognized as dominant (Frank et al., 2001), increased the *petite* frequency in an heteroallelic diploid mutant strain (Nasca et al., 2016). The significant increase (3.3-fold±0.6, $p<0.001$) of the *petite* frequency observed, compared to the hemizygous strain, suggests that also the Gly252Val mutation behaves as partially dominant, at least for this specific phenotype (**Figure 8D**).

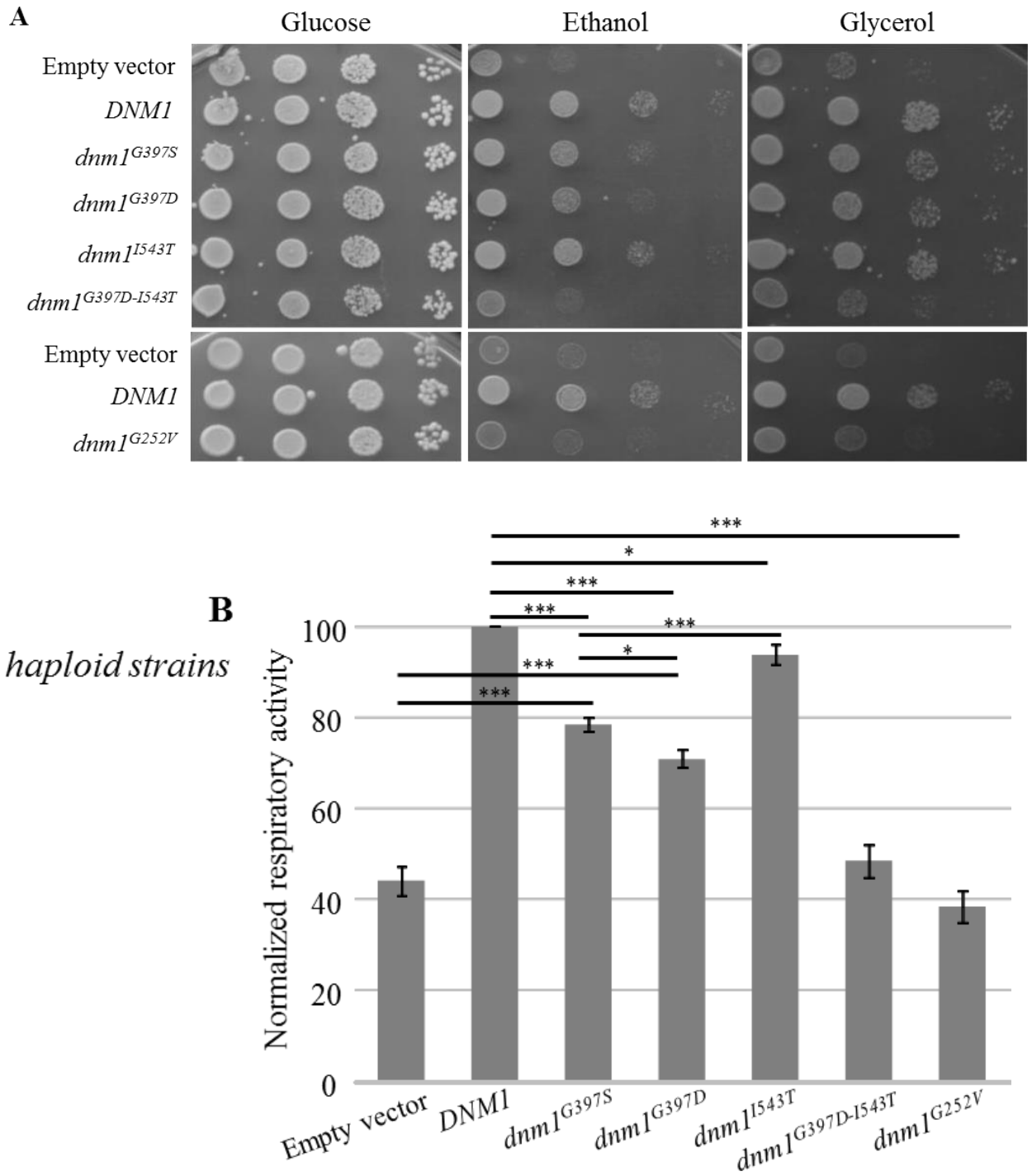

Figure 8: **Functional study in yeast.** (A) Phenotypic analysis of haploid strains through spot assay. Serial cell dilutions of dnm1Δ haploid strain transformed with DNM1 wt or mutant alleles were spotted on Synthetic complete medium supplemented with either 2% glucose or 2% glycerol. (B) Respiratory activity of dnm1Δ haploid strain transformed with DNM1 wt or mutant alleles. *($p<0.05$), **($p<0.01$) and ***($p<0.001$).

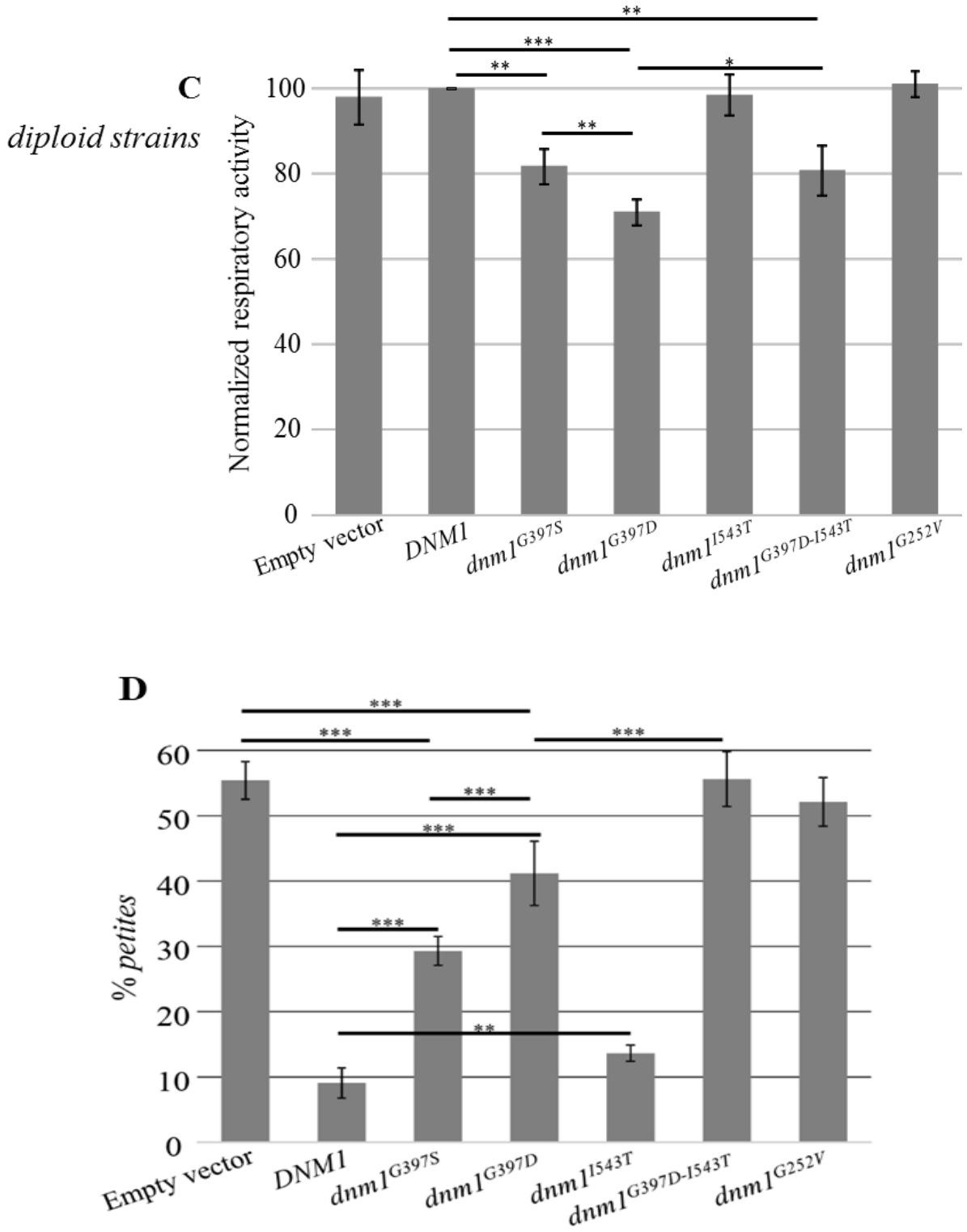

Figure 8: **Functional study in yeast.** (C) Respiratory activity of DNM1/dnm1Δ diploid strain transformed with DNM1 wt or mutant alleles. (D) *petite* frequency of DNM1/dnm1Δ diploid strain transformed with DNM1 wt or mutant alleles. *($p<0.05$), **($p<0.01$) and ***($p<0.001$).

Structural analysis

All the identified missense mutations affect sites, which are totally or highly conserved sites among species (**Figure 9A**) and imply replacements with residues presenting physicochemical properties that differ significantly from those of the wild type amino acids. The Gly223Val mutation causes the substitution of the tiny and flexible glycine with a hydrophobic valine, which is expected to induce structural changes in the GTPase domain near residues 215-221 important for the binding of GTP (**Figure 9B**). The Gly362Asp and Gly362Ser mutations replace the tiny glycine with the anionic aspartic acid or with the hydrophilic serine, respectively, modifying the N-terminus of an α-helix also exploited in dynamin tetramerization (**Figure 9C**), as inferred by homology of dynamin-1-like with dynamin 3, another member of the dynamin family. The Phe370Cys mutation affects the large and hydrophobic phenylalanine that is important for the stability of monomers and for the tetramer formation (**Figure 9D**). In fact, Phe370 is involved in several intramolecular hydrophobic interactions, which are disrupted by the replacement with the small cysteine and the latter might also become engaged in disulfide bond formation with other cysteines located nearby. The Arg403Cys mutation implies the change of the cationic arginine into the tiny and neutral cysteine at sites that contribute to the core of tetrameric dynamin assembly (**Figure 9E**), as previously reported (Fahrner et al., 2016).

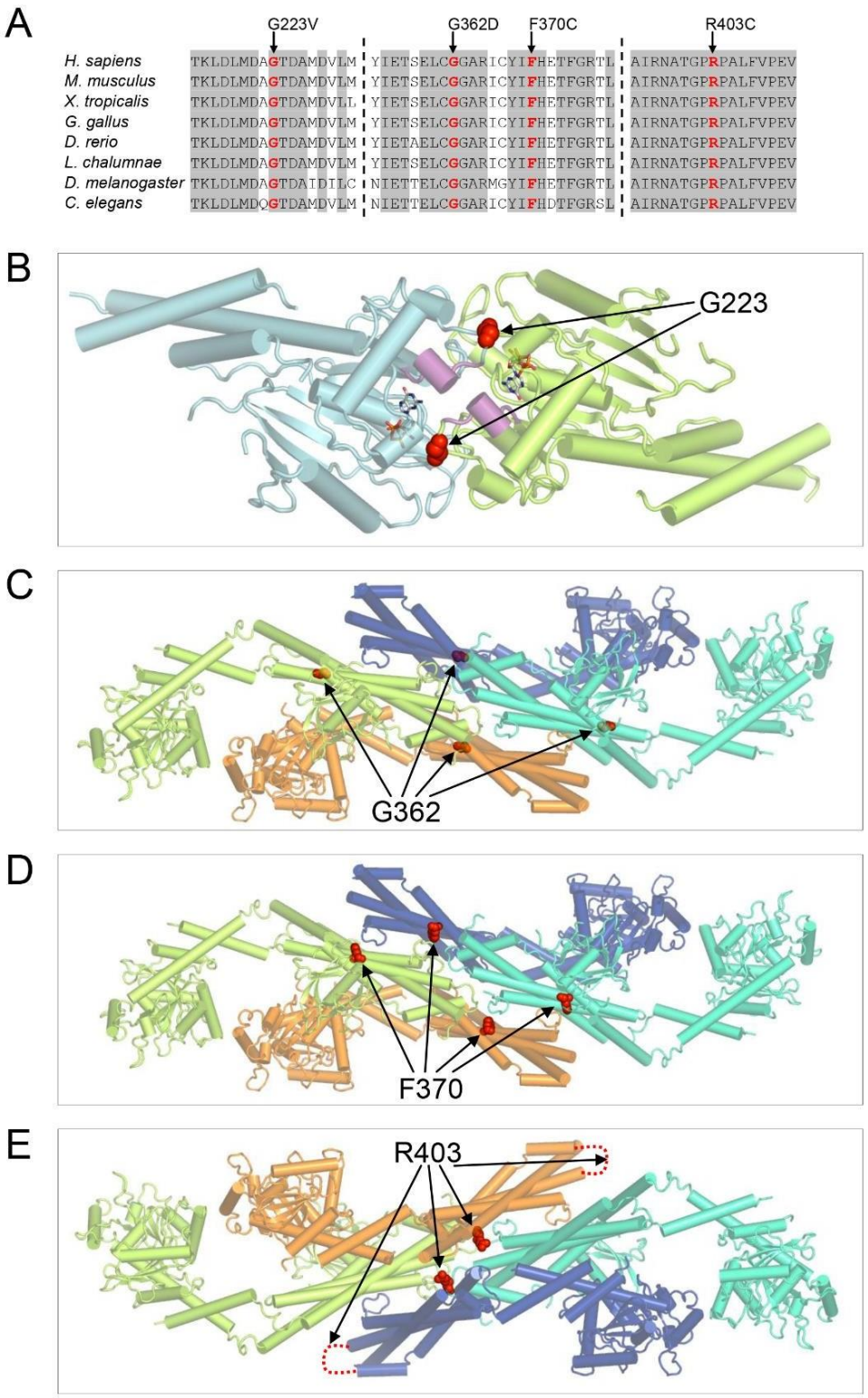

Figure 9: Conservation and structural mapping of residues affected by the missense mutations G223V, G362D, F370C, and R403C. (A): multiple sequence alignment among species (invariant columns are grayed). Structural mapping of residues affected by the missense mutations G223V, G362D, F370C, and R403C. Mapping of G223 (B) on the crystal structure of a dimeric human dynamin- 1-like protein (PDB 3W6O). Mapping of G362 (C), F370 (D), and R403 (E) on dynamin tetramer (PDB 5A3F).

Discussion

The use of NGS technology allowed us to described four patients with *de novo* dominant missense mutations in *DNM1L*. All the patients presented some classical features of mitochondrial disease such as early symptoms of encephalopathy, developmental delay, drug resistant seizures and, only in Pt.2 and Pt.5, blood lactic acidemia.

We identified two novel variants in Pt.1 and Pt.3, whereas in Pt.2 and Pt.5 we found two variants that were already reported (Fahrner *et al*., 2016; Sheffer *et al*., 2015). Pt.4 showed two variants on the same allele; the first was inherited from the mother and the second, recently described as a *de novo* mutation (Vanstone et al., 2016), was present in the mother's blood DNA at low level (~5%), suggesting a maternal mosaicism. We observed a quite strict genotype-phenotype correlation, with overlapping clinical presentations between Pt.2, Pt.4, Pt.5 and the previously described patients harboring the same mutation (reported by Fahrner *et al*., Vanstone *et al*. and Sheffer *et al*., respectively).

Following the first description of Waterham *et al*., there have been increasing reports in the last 2 years on patients, frequently sporadic, with *de novo* dominant-negative *DNM1L* mutations who are affected by early onset encephalopathy with microcephaly and drug resistant seizures, progressive brain atrophy or abnormal brain development, optic atrophy, and occasionally persistent lactic acidemia (Fahrner *et al*., 2016; Schmid *et al*., 2019; Sheffer *et al*., 2015; Longo *et al*.2019). The patients described here presented clinical manifestations quite similar to previously reported *DNM1L* cases.

Probably the most peculiar finding in the cohort of our patients is the muscle histology/histochemistry showing core like areas using oxidative enzyme staining for COX and SDH, which suggest an abnormal distribution of mitochondria in the muscle tissue. We found this pattern in all the examined muscle biopsies. Moreover, in serial sections of muscle fibers of Pt.3 we demonstrated that the fibers that are no reactive for COX, SDH and NADH are also negative for the staining with ATPase 9.4 indicating that these are type I muscular fibers. In addition, the EM in Pt.4 showed enlarged mitochondria, sometimes two mitochondria were coupled and appeared to be in close relationship to each other. Areas devoted of mitochondria has not been found in muscle biopsies of *OPA1* mutated patients that, sometimes, showed ragged red-COX negative fibers correlated with mitochondrial DNA instability (Amati- Bonneau et al., 2008). Our findings are new for *DNM1L* patients; in fact, no histochemical alteration has ever been reported, and only once abnormalities in mitochondrial cristae were

observed (Vanstone et al., 2016).
At the cellular level, using fluorescence microscopy, we found the presence of hyperfused, swollen and rod-shaped mitochondria in fibroblasts from all our patients, as reported for others *DNM1L* mutations (Waterham et al., 2007, Fahrner et al., 2016; Zaha et al., 2016; Sheffer et al., 2016; Vanstone et al., 2016; Nasca et al., 2016; Gerber et al., 2017; Longo *et al*.2019). The morphological anomalies were not associated with OXPHOS dysfunctions, in fact we did not observe reduction of OXPHOS subunits levels. The same findings have been reported in most of the *DNM1L*-mutant cases. Moreover, these results are consistent with the one obtained in muscle sample, in which the activities of the respiratory chain complexes were also normal.
In addition to mitochondrial fission, DRP1 is also implicated in the peroxisomes' division (Schrader et al., 2016); to this purpose we investigated peroxisomal morphology and in fibroblasts from Pt. 4 and Pt. 5 we observed organelles longer, larger, and less uniformly distributed into cytoplasm, in contrast with the highly diffused punctuated staining present in control cells; the same condition has been described for other patients with mutations in *DNM1L* (Waterham et al., 2007; Nasca et al., 2016; Zaha et al., 2016).
DRP1 protein consists of four conserved regions: the GTPase domain, the middle, the variable, and the GTPase effector domain (GED). In the cytosol, DRP1 exists as a mixture of dimers and tetramers (Macdonald et al., 2014) and, when recruited to mitochondria via receptors anchored to the mitochondrial outer membrane (Losón et al., 2013), hydrolysis of GTP triggers conformational changes in DRP1 oligomers that generate the mechanical force to promote mitochondrial membrane scission (Francy et al., 2015). The middle and GED domains promote DRP1 self-assembly, required for mitochondrial fission (Chang et al., 2010), while the variable domain seems to act as a negative regulator of DRP1 self-assembly (Francy et al., 2015).
We noted that mutations that fall into the GTPase domain are typically associated with a recessive trait, except for the cases not associated with early encephalopathy, reported by Gerber et al., 2017, while mutations that fall into the middle domain are expressed as dominant- negative. In only one of our patients (Pt. 1) we identified a mutation (p.Gly223Val) which falls into the GTPase domain, even if the nucleotide exchange is located at the boundary between the GTPase and the central domain.
Using the *in silico* structural model we demonstrated that the Gly223Val (Pt.1) mutation induces structural changes in the GTPase domain; while the remaining

mutations affect the stability of monomers and the tetramer formation.
Finally, the *S. cerevisiae* model confirmed the pathogenicity of all variants. Moreover, we demonstrated for all the mutations a dominant negative effect and that the second mutation (p.Ile512Thr) of the Pt.4 act as a modifier, able to worsen the phenotype associated with the p.Gly362Asp mutation.
In conclusion, in this part of this thesis, we have described six variants in *DNM1L* gene, two of which has never been reported. Also, we confirmed their pathogenicity and expanded the spectrum of the mutations occurring in this gene; finally, we observed for the first time a peculiar alteration in muscle specimen never associated before with mutations in *DNM1L*.

Methods

Standard protocol approvals, registrations and patients consents

The study was approved by the Ethical Committees of the Bambino Gesù Children's Hospital, Rome, Italy, and the C. Besta Neurological Institute, Milan, Italy, in agreement with the Declaration of Helsinki.

Histological, ultrastructural and biochemical analyses

Cryostatic cross-sections of quadriceps muscle biopsies were processed according to standard histochemical and immunohistochemical procedures. Respiratory chain complexes (RCCs) activities were assayed in muscle homogenate and normalized to citrate synthase activity, using a previously reported spectrophotometric method (Bugiani et al., 2004). For ultrastructural studies, muscle specimens were fixed in 2.5% glutaraldehyde in 0.1 M cacodylate buffer (pH 7.4) at 4°C. Samples were post-fixed with 2% OsO4 in 0.1 M cacodylate buffer (pH 7.4) for 1

h. Specimens were dehydrated in a graded series of ethanol and embedded in epon resin. Thin sections were evaluated with a transmission electron microscope (EM 109 Zeiss) (Fattori et al., 2018).

Mutational analysis

Genomic DNA was isolated from blood and cultured skin fibroblasts using QIAamp DNA mini kit (QIAGEN, Valencia, CA, USA). DNA from Pt.1, Pt.2 and Pt.3 underwent high-throughput sequencing by TruSight One panel (Illumina, San Diego, CA) comprehensive of > 4.800 clinically relevant genes. The enrichment was achieved following manufacture instruction and the sequencing analysis was performed on MiSeq System. Variant-Studio software was applied for analysis, classification, and reporting of genomic variants. After excluding previously annotated single nucleotide changes occurring with high frequency in populations (>1%), we prioritized variants predicted to have functional impact (i.e. nonsynonymous variants and changes affecting splice sites). Pt.4 and Pt.5 were analyzed using a custom gene panel for the screening of 224 genes associated with mitochondrial diseases (Ardissone et al., 2018). Sanger sequencing was used to validate all the annotated functionally relevant variants, as well as to check variant segregation in the families. Bioinformatics tools based on heuristic methods, SIFT (http://sift.jcvi.org) and PolyPhen-2 (http://genetics.bwh.harvard.edu/pph2), were used for pathogenicity prediction of the variants**.**

Western blotting analysis and antibodies

For SDS-PAGE, 40 μg of fibroblasts homogenate were loaded in a 12%

denaturating gel. Western blot (WB) was achieved by transferring proteins onto polyvinylidene difluoride (PVDF) membrane and probed with specific antibodies. Specific bands were detected using Lite A blot Extend Long Lasting Chemiluminescent Substrate (Euroclone, Pero (Mi), Italy). Densitometry analysis was performed using Quantity One software (BioRad, Hercules, CA, USA).
RCC subunits were detected using the following monoclonal antibodies purchased from MitoScience (Eugene, OR, USA): Complex I – NDUFA9; complex II – SDHB; complex IV – COXII; Complex V – ATP5B; porin (VDAC). Polyclonal rabbit GAPDH (Sigma-Aldrich), monoclonal antibody OPA1 (BD Biosciences) and DRP1 (Abcam) were also used.

Tissue culture, Immunostaining and Imaging

Human fibroblasts were obtained from a diagnostic skin biopsy and grown in DMEM medium supplemented with 10% fetal bovine serum, 4.5 g/L glucose, and 50 μg/mL uridine**.**
To display the mitochondrial network arrangement, fibroblasts from Pt.1, Pt.2, Pt.3 were fixed and permeabilized using methanol:acetone (2:1) for 10 min at room temperature, then a blocking solution containing 5% BSA in PBS was used. The polyclonal rabbit TOMM20 antibody (Santa Cruz Biotechnology) was applied overnight and visualized using Alexa Fluor 647 secondary antibody (Jackson Immuno Research), both antibodies were used at the dilution of 1:500. Images were acquired with a fluorescence-inverted microscope (Leica DMi8). An average of 8 image planes was obtained along the z-axis at 0.2 μm increments using LASX
3.0.4 (Leica) software. Mitochondrial depolarization was induced using 20 μM protonophore carbonyl cyanide m-chlorophenyl hydrazine (CCCP) for 3 hours. For Pt.4 and Pt.5 the mitochondrial network was visualized in living cells using the mitochondrial fluorescent dye MitoTracker Red-CMXRos (Invitrogen) at final concentrations of 50 nM for 30 min; then images were acquired with a confocal microscope (Leica TSC-SP8). For peroxisomal immunostaining we used the polyclonal rabbit PMP70 antibody (Sigma-Aldrich) applied overnight at the concentration of 1:200, followed by Alexa Fluor 488 secondary antibody (1:500). The peroxisomal staining was visualized using the same parameters used above.

Statistical analysis

For each experiment, data obtained were calculated as the mean of replicates ± standard deviation (SD).

Structural analysis

The residues affected by the missense mutations described in this work

(p.Gly223Val, p.Gly362Asp, p.Phe370Cys, and p.Arg403Cys) were mapped on crystal structures of homologues proteins. The crystal structure of a dimeric human dynamin-1-like protein (Protein Data Bank, PDB, 3W6O) was used for the p.Gly223Val mutation. The crystal structure of the Dynamin-3 tetramer (PDB 5A3F) was used for the p.Gly362Asp, p.Phe370Cys, and p.Arg403Cys mutations. The cryo-electron microscopy structure of human dynamin-1 co- assembled with MID49 (PDB 5WP9) was used to obtain the detailed view of the site of the p.Phe370Cys mutation. Molecular structures were rendered with PyMOL (http://www.pymol.org).

Functional studies in yeast

Yeast strains and media. The yeast strains used in this work were the haploid strain W303-1B (*MATa leu2-3, trp1-1, can1-100, ura3-1, ade 2-1, his3-11*) and its isogenic strain *dnm1*::KanR, and the hemizygous diploid strain W303 *dnm1*_ (*MATa*/*MAT**a*** *leu2-3/leu2-3, trp1-1/trp1-1, can1- 100/can1-100, ura3-1/ura3-1, ade 2-1/ade2-1, his3-11/his3-11 DNM1/dnm1*::KanR). All experiments were performed in Synthetic complete medium (SC, 6.9 g/l yeast nitrogen base without amino acids (ForMedium), 1 g/l drop-out mix without amino acids or bases necessary to keep plasmids) (Kaiser et al., 1994). Media were supplemented with carbon sources (Carlo Erba Reagents) as indicated in the text in liquid phase or after solidification with 20g/L agar (ForMedium). Construction of *dnm1* mutant strains. *dnm1* mutant alleles and *dnm1* mutant strains were
constructed as previously reported (Nasca et al., 2016). Briefly, *dnm1* mutant alleles were constructed using mutagenic overlap PCR with the oligonucleotides reported in Supplementary Table S1, digested with *Bam*HI and *Xba*I or *Xba*I and *Sal*I, and subcloned in pFL38DNM1. In order to obtain haploid wild type or mutant strains all plasmids were introduced by transformation in the W303-1B *dnm1'* haploid strain and in the W303 *dnm1'* hemizygous diploid strain using the "LiAc/SS carrier DNA/PEG quick method" as previously reported (Gietz & Woods, 2002). Yeast analyses. Spot assay was performed by spotting 5x104, 5x103, 5x102 and 5x101 cells on SC supplemented with different carbon sources. *Petite* frequency was measured as previously reported (Baruffini et al., 2010) in six to eight independent clones for each strain. Oxygen consumption rate was measured in SC medium as previously described (Goffrini et al., 2009) on five independent clones, after growth in conditions, which minimized the *petite* frequency, which was lower than 5%. (Nolli et al., 2015). All experiments were performed at 37°C, except for the measurement of the *petite* frequency in the diploid strains, which was performed at 28°C

References general introduction, summary and aims:

Campello, S. and Scorrano, L. (2010) 'Mitochondrial shape changes: Orchestrating cell pathophysiology', EMBO Reports, 11(9), pp. 678–684.

Craven L, Alston CL, Taylor RW, Turnbull DM. (2017) 'Recent Advances in Mitochondrial Disease', Annu Rev Genomics Hum Genet. Aug 31;18:257-275.

Gorman GS, Chinnery PF, DiMauro S, Hirano M, Koga Y, McFarland R, Suomalainen A, Thorburn DR, Zeviani M, Turnbull DM. (2016) 'Mitochondrial diseases', Nat Rev Dis Primers. Oct 20;2:16080.

Ghezzi, D. and Zeviani, M. (2018) 'Human diseases associated with defects in assembly of OXPHOS complexes', Essays in Biochemistry, pp. 271–286.

Matsushima, Y. and Kaguni, L. S. (2012) 'Matrix proteases in mitochondrial DNA function', Biochimica et Biophysica Acta - Gene Regulatory Mechanisms. Elsevier B.V., 1819(9–10), pp. 1080–1087.

Nimmo, G. A. M. et al. (2019) 'Bi-Allelic mutations of LONP1 encoding the mitochondrial LonP1 protease cause pyruvate dehydrogenase deficiency and profound neurodegeneration with progressive cerebellar atrophy', Human Molecular Genetics, 28(2), pp. 290–306.

Peter, B. et al. (2018) 'Defective mitochondrial protease LonP1 can cause classical mitochondrial disease', Human Molecular Genetics, 27(10), pp. 1743–1753.

Schmid, S. J. et al. (2019) 'A de Novo Dominant Negative Mutation in DNM1L Causes Sudden Onset Status Epilepticus with Subsequent Epileptic Encephalopathy', Neuropediatrics, 50(3), pp. 197–201.

Stenton SL, Prokisch H. (2018) 'Advancing genomic approaches to the molecular diagnosis of mitochondrial disease', Essays Biochem. Jul 20;62(3):399-408.

Suomalainen, A. and Battersby, B. J. (2018) 'Mitochondrial diseases: The contribution of organelle stress responses to pathology', Nature Reviews Molecular Cell Biology. Nature Publishing Group, pp. 77–92.

References

Amati-Bonneau P, Valentino ML, Reynier P, Gallardo ME, Bornstein B, Boissière A, Campos Y, Rivera H, de la Aleja JG, Carroccia R, Iommarini L, Labauge P, et al. 2008. OPA1 mutations induce mitochondrial DNA instability and optic atrophy 'plus' phenotypes. Brain. 131:338-351.

Anikster, Y., Kleta, R., Shaag, A., Gahl, W. A., & Elpeleg, O. (2001). Type III 3-methylglutaconic aciduria (optic atrophy plus syndrome, or Costeff optic atrophy syndrome): identification of the OPA3 gene and its founder mutation in Iraqi

Jews. The American Journal of Human Genetics, 69(6), 1218-1224.

Ardissone A, Tonduti D, Legati A, Lamantea E, Barone R, Dorboz I, Boespflug-Tanguy O, Nebbia G, Maggioni M, Garavaglia B, Moroni I, Farina L, et al. 2018. KARS-related diseases: progressive leukoencephalopathy with brainstem and spinal cord calcifications as new phenotype and a review of literature. Orphanet J Rare Dis 13:45.

Bartsakoulia M, Pyle A, Troncoso-Chandía D, Vial-Brizzi J, Paz-Fiblas MV, Duff J, Griffin H, Boczonadi V, Lochmüller H, Kleinle S, Chinnery PF, Grünert S, et al. 2018. A novel mechanism causing imbalance of mitochondrial fusion and fission in human myopathies. Hum Mol Genet 27:1186-1195

Baruffini E, Ferrero I, and Foury F. 2010. In vivo analysis of mtDNA replication defects in yeast. Methods 51:426-436. Manual, Cold Spring Harbor Laboratory Press, Cold Spring Harbor, NY.

Bernhardt D, M¨uller M, Reichert AS, Osiewacz HD. 2015. Simultaneous impairment of mitochondrial fission and fusion reduces mitophagy and shortens replicative lifespan. Sci Rep 5:7885.

Bugiani M, Invernizzi F, Alberio S, Briem E, Lamantea E, Carrara F, Moroni I, Farina L, Spada M, Donati MA, Uziel G, Zeviani M. 2004. Clinical and molecular findings in children with complex I deficiency. Biochim Biophys Acta 1659:136-1347.

Cagliani R, Fruguglietti ME, Berardinelli A, D'Angelo MG, Prelle A, Riva S, Napoli L, Gorni K, Orcesi S, Lamperti C, Pichiecchio A, Signaroldi E, et al. 2011. New molecular findings in congenital myopathies due to selenoprotein N gene mutations. J Neurol Sci. 300:107-13.

Cahill TJ, Leo V, Kelly M, Stockenhuber A, Kennedy NW, Bao L, Cereghetti GM, Harper AR, Czibik G, Liao C, Bellahcene M, Steeples V, et al. 2016. Resistance of dynamin-related protein 1 oligomers to disassembly impairs mitophagy, resulting in myocardial inflammation and heart failure. J Biol Chem 291:25762.

Chang CR, Manlandro CM, Arnoult D, Stadler J, Posey AE, Hill RB, Blackstone C. 2010. A lethal de novo mutation in the middle domain of the dynamin-related GTPase Drp1 impairs higher order assembly and mitochondrial division. J Biol Chem 285:32494-32503.

Chao YH, Robak LA, Xia F, Koenig MK, Adesina A, Bacino CA, Scaglia F, Bellen HJ, Wangler MF. 2016. Missense variants in the middle domain of

DNM1L in cases of infantile encephalopathy alter peroxisomes and mitochondria when assayed in Drosophila. Hum Mol Genet 25:1846-1856.

Chung, K. W., Kim, S. M., Sunwoo, I. N., Cho, S. Y., Hwang, S. J., Kim, J., Kang SH, Park KD, Choi KG, Choi SI, Choi, B. O. (2008). A novel GDAP1 Q218E mutation in autosomal dominant Charcot-Marie-Tooth disease. Journal of human genetics, 53(4), 360.

Fahrner JA, Liu R, Perry MS, Klein J, Chan DC. 2016. A novel de novo dominant negative mutation in DNM1L impairs mitochondrial fission and presents as childhood epileptic encephalopathy. Am J Med Genet A 170:2002-2011.

Fattori F, Fiorillo C, Rodolico C, Tasca G, Verardo M, Bellacchio E, Pizzi S, Ciolfi A, Fagiolari G, Lupica A, Broda P, Pedemonte M, et al. 2018. Expanding the histopathological spectrum of CFL2- related myopathies. Clin Genet 93:1234-1239.

Francy CA, Alvarez FJ, Zhou L, Ramachandran R, Mears JA. 2015. The mechanoenzymatic core of dynamin-related protein 1 comprises the minimal machinery required for membrane constriction. J Biol Chem 290:11692-11703.

Frank S, Gaume B, Bergmann-Leitner ES, LeitnerWW, Robert EG, Catez F, Smith CL, Youle RJ. 2001. The role of dynamin-related protein 1, a mediator of mitochondrial fission, in apoptosis. Dev Cell 1:515–525.

Gerber S, Charif M, Chevrollier A, Chaumette T, Angebault C, Kane MS, Paris A, Alban J, Quiles M, Delettre C, Bonneau D, Procaccio V, et al. 2017. Mutations in DNM1L, as in OPA1, result in dominant optic atrophy despite opposite effectson mitochondrial fusion and fission. Brain. 140:2586-2596.

Gietz RD, Woods RA. 2002. Transformation of yeast by the LiAc/SS carrier DNA/Peg method. Methods in Enzymology 350: 87-96.

Goffrini P, Ercolino T, Panizza E, Giachè V, Cavone L, Chiarugi A, Dima V, Ferrero I. Mannelli M. 2009. Functional study in a yeast model of a novel succinate dehydrogenase subunit B gene germline missense mutation (C191Y) diagnosed in a patient affected by a glomus tumor. Hum. Mol. Genet 18:1860-1868.

Horbay, R. and Bilyy, R. 2016. Mitochondrial dynamics during cell cycling, Apoptosis. Springer US, 21(12), pp. 1327–1335.

Ishihara N, Nomura M, Jofuku A, Kato H, Suzuki SO, Masuda K, Otera H, Nakanishi Y, Nonaka I, Goto Y, Taguchi N, Morinaga H, et al. 2009.

Mitochondrial fission factor Drp1 is essential for embryonic development and synapse formation in mice. Nat Cell Biol 11:958-966.

Kageyama Y, Zhang Z, Roda R, Fukaya M, Wakabayashi J, Wakabayashi N, Kensler TW, Reddy PH, Iijima M, Sesaki H. 2012. Mitochondrial division ensures the survival of postmitotic neurons by suppressing oxidative damage. J Cell Biol 197:535-551.

Kaiser C, Michaelis S, Mitchell A. 1994. Methods in Yeast Genetics: a Laboratory Course.

Koch J, Feichtinger RG, Freisinger P, Pies M, Schr¨odl F, Iuso A, Sperl W, Mayr JA, Prokisch H,Haack TB. 2016. Disturbed mitochondrial and peroxisomal dynamics due to loss of MFF causes Leigh-like encephalopathy, optic atrophy and peripheral neuropathy. J Med Genet 53:270–278.

Lenaers G, Hamel C, Delettre C, Amati-Bonneau P, Procaccio V, Bonneau D, Reynier P, Milea D. 2012. Dominant optic atrophy. Orphanet J Rare Dis 7:46.

Li Z, Okamoto K, Hayashi Y, Sheng M. 2004. The importance of dendritic mitochondria in the morphogenesis and plasticity of spines and synapses. Cell 119:873-887.

Longo F, Benedetti S, Zambon AA, Sora MGN, Di Resta C, De Ritis, D., ... & Previtali, S. C. (2019). Impaired turnover of hyperfused mitochondria in severe axonal neuropathy due to a novel DRP1 mutation. Human Molecular Genetics.

Longo, F., Benedetti, S., Zambon, A. A., Sora, M. G. N., Di Resta, C., De Ritis, D, Quattrini A., Maltecca F., Ferrrari M., Previtali, S. C. (2019). Impaired turnover of hyperfused mitochondria in severe axonal neuropathy due to a novel DRP1 mutation. Human Molecular Genetics.

Losón OC, Song Z, Chen H, Chan DC. 2013. Fis1, Mff, MiD49, and MiD51 mediate Drp1 recruitment in mitochondrial fission. Mol Biol Cell 24:659-667.

Macdonald PJ, Stepanyants N, Mehrotra N, Mears JA, Qi X, Sesaki H, Ramachandran R. 2014. A dimeric equilibrium intermediate nucleates Drp1 reassembly on mitochondrial membranes for fission. Mol Biol Cell. 25:1905-1915.

Nasca A, Legati A, Baruffini E, Nolli C, Moroni I, Ardissone A, Goffrini P, Ghezzi D. 2016. Biallelic Mutations in DNM1L are Associated with a Slowly Progressive Infantile Encephalopathy. Hum Mutat 37:898-903.

Nasca A, Rizza T, Doimo M, Legati A, Ciolfi A, Diodato D, Calderan C, Carrara G, Lamantea E, Aiello C, Di Nottia M, Niceta M, et al. 2017. Not only dominant, not only optic atrophy: expanding the clinical spectrum associated with OPA1 mutations. Orphanet J Rare Dis 12:89.

Nasca A, Scotton C, Zaharieva I, Neri M, Selvatici R, Magnusson OT, Gal A, Weaver D, Rossi R, Armaroli A, Pane M, Phadke R, et al. 2017. Recessive mutations in MSTO1 cause mitochondrial dynamics impairment, leading to myopathy and ataxia. Hum Mutat 38:970-977

Nolli C, Goffrini P, Lazzaretti M, Zanna C, Vitale R, Lodi T, Baruffini E. 2015. Validation of a MGM1/OPA1 chimeric gene for functional analysis in yeast of mutations associated with dominant optic atrophy. Mitochondrion 25:38-48.

Otsuga D, Keegan BR, Brisch E, Thatcher JW, Hermann GJ, Bleazard W, Shaw JM. 1998. The dynamin-related GTPase, Dnm1p, controls mitochondrial morphology in yeast. J Cell Biol 143:333- 349.

Pagliuso, A., Cossart, P. and Stavru, F. (2018) 'The ever-growing complexity of the mitochondrial fission machinery', Cellular and Molecular Life Sciences. Springer International Publishing, 75(3), pp. 355–374.

Pitts KR, McNiven MA, Yoon Y. 2004. Mitochondria-specific function of the dynamin family protein DLP1 is mediated by its C-terminal domains. J Biol Chem 279:50286-94.

Rapaport D, Brunner M, Neupert W, Westermann B. 1998. Fzo1p is a mitochondrial outer membrane protein essential for the biogenesis of functional mitochondria in Saccharomyces cerevisiae. J Biol Chem 273:20150–20155.

Santel A, Fuller MT. Control of mitochondrial morphology by a human mitofusin. 2001. J Cell Sci 114:867-874.

Schmid, S. J. et al. (2019) 'A de Novo Dominant Negative Mutation in DNM1L Causes Sudden Onset Status Epilepticus with Subsequent Epileptic Encephalopathy', Neuropediatrics, 50(3), pp. 197–201.

Schrader M, Costello JL, Godinho LF, Azadi AS, Islinger M. 2016. Proliferation and fission of peroxisomes - An update. Biochim Biophys Acta 1863:971-983.

Sesaki H, Southard SM, Yaffe MP, Jensen RE. 2003. Mgm1p, a dynamin-related GTPase, is essential for fusion of the mitochondrial outer membrane. MolBiolCell 14:2342–2356.

Sewry CA, Müller C, Davis M, Dwyer JS, Dove J, Evans G, Schröder R, Fürst D, Helliwell T, Laing N, Quinlivan RC. 2002. The spectrum of pathology in central core disease. Neuromuscul Disord. 10:930-938.

Shamseldin HE, Alshammari M, Al-Sheddi T, SalihMA, AlkhalidiH,Kentab A, Repetto GM, Hashem M, Alkuraya FS. 2012. Genomic analysis of mitochondrial diseases in a consanguineous population reveals novel candidate disease genes. J Med Genet 49:234–241.

Sheffer R, Douiev L, Edvardson S, Shaag A, Tamimi K, Soiferman D, Meiner V, Saada A. 2016. Postnatal microcephaly and pain insensitivity due to a de novo heterozygous DNM1L mutation causing impaired mitochondrial fission and function. Am J Med Genet A 170:1603-1607.

Sheng ZH, Cai Q. 2012. Mitochondrial transport in neurons: impact on synaptic homeostasis and neurodegeneration. Nat Rev Neurosci 13:77-93.

Sheng ZH. 2017. The Interplay of Axonal Energy Homeostasis and Mitochondrial Trafficking and Anchoring. Trends Cell Biol 27:403-416.

Stuppia G, Rizzo F, Riboldi G, Del Bo R, Nizzardo M, Simone C, Comi GP, Bresolin N, Corti S. MFN2-related neuropathies: Clinical features, molecular pathogenesis and therapeutic perspectives. 2015. J Neurol Sci 356:7-18.

ten Brink HJ, Schor DS, Kok RM, Poll-The BT, Wanders RJ, Jakobs C. 1992. Phytanic acid alpha- oxidation: accumulation of 2-hydroxyphytanic acid and absence of 2-oxophytanic acid in plasma from patients with peroxisomal disorders. J Lipid Res 33:1449-1457.

Valente AJ, Fonseca J, Moradi F, Foran G, Necakov A, Stuart JA. Quantification of Mitochondrial Network Characteristics in Health and Disease. Adv Exp Med Biol. 2019; 1158:183-196.

Vanstone JR, Smith AM, McBride S, Naas T, Holcik M, Antoun G, Harper ME, Michaud J, Sell E, Chakraborty P, Tetreault M, Care4Rare Consortium, et al. 2016. DNM1L-related mitochondrial fission defect presenting as refractory epilepsy. Eur J Hum Genet 24:1084-1088.

Wakabayashi J, Zhang Z, Wakabayashi N, Tamura Y, Fukaya M, Kensler TW, Iijima M, Sesaki H. 2009. The dynamin-related GTPase Drp1 is required for embryonic and brain development in mice. J Cell Biol 186:805-816.

Waterham HR, Koster J, van Roermund CW, Mooyer PA, Wanders RJ, Leonard JV. 2007. A lethal defect of mitochondrial and peroxisomal fission. N Engl J Med

356:1736–1741.

Yoon G, Malam Z, Paton T, Marshall CR, Hyatt E, Ivakine Z, Scherer SW, Lee KS, Hawkins C, Cohn RD; Finding of Rare Disease Genes (FORGE) in Canada Consortium Steering Committee, 2016. Lethal disorder of mitochondrial fission caused by mutations in DNM1L. J Pediatr 171:313– 316.

Youle RJ, van der Bliek AM. 2012. Mitochondrial fission, fusion, and stress. Science 337:1062- 1065.

Yu-Wai-Man P, Griffiths PG, Gorman GS, Lourenco CM, Wright AF, Auer-GrumbachM, Toscano A, Musumeci O, Valentino ML, Caporali L, Lamperti C, Tallaksen CM, et al. 2010 Multi-system neurological disease is common in patients with OPA1 mutations. Brain 133:771-786.

Zaha K, Matsumoto H, Itoh M, Saitsu H, Kato K, Kato M, Ogata S, Murayama K, Kishita Y, Mizuno Y, Kohda M, Nishino I, et al. 2016. DNM1L-related encephalopathy in infancy with Leigh syndrome-like phenotype and suppression-burst. Clin Genet 90:472-474.

Zanna C, Ghelli A, Porcelli AM, Karbowski M, Youle RJ, Schimpf S, Wissinger B, Pinti M, Cossarizza A, Vidoni S, Valentino ML, Rugolo M, et al. 2008. OPA1 mutations associated with dominant optic atrophy impair oxidative phosphorylation and mitochondrial fusion. Brain 131:352- 367.

II PART

Introduction

Lon is a 959-residue long serine protease, encoded by the nuclear gene, *LONP1*, conserved among prokaryotes and eukaryotes; it belongs to the AAA+ protein family (ATPases Associated with a wide variety of cellular Activities) and is one of the main actors of the mitochondrial quality control. The protein is composed of four distinct domains: the mitochondrial target sequencing domain (MTS) which direct the localization of Lon to the mitochondrial matrix, the substrate recognition domain, the ATPase domain which bind ATP and the proteolytic domain (**Fig.9A**). The structure of Lon in human has been solved by X-ray crystallography only for the proteolytic domain and it has been observed that it has the same structural layout of bacterial and archaeal Lon protease, showing an active site with a Ser-Lys dyad (S855-K898). In its activated state Lon forms a quaternary structure as a homo-hexamer in which ATPase and proteolytic domains occupy the head region of the hexamer while the substrate binding domain the leg's region (**Fig.9B**). The proteolytic activity of Lon is driven by conformational changes resulting from the binding and hydrolysis of ATP, mediated by its ATPase domain.

The maintenance of mitochondrial health and function is provided by a set of chaperones and proteases, located in different mitochondrial compartments, which control the biosynthesis, folding or degradation of misfolded proteins. The AAA+ proteases are specifically located as follow: in the mitochondrial matrix are present Lon and the ClpXP (Caseinolytic Mitochondrial Matrix Peptidase) complex, in the IMM the intermembrane the (i-AAA) protease YMEIL1L, and the AFGL3L2 and paraplegin are inserted into the IMM and facing the matrix.

Lon, in the mitochondrial matrix, acts mainly as a protease but also as a chaperone to guide the folding of several respiratory chain complexes subunits (Rep *et al.*, 1996). Moreover, it can regulate the stability of the mtDNA, directly binding it (Fu, Smith & Markovitz, 1997; Fu & Markovitz,1998) or indirectly regulating the degradation of the main transcription factor of the mtDNA, TFAM (Lu *et al.*, 2007). Several experiments have shown the functional involvement of the Lon protein in ageing, as well as in tumorigenic transformation (Luciakova *et al.*, 1999; Luce and Osiewacz, 2012).

LONP1 mutations have been associated to a severe disease, known as CODAS (Cerebral, Ocular, Dental, Auricular, Skeletal anomalies) (Shebib *et al.*, 1991; Strauss *et al.*, 2015) (OMIM #600373). Only recently *LONP1* mutations have been recognized as the genetic cause of a subtype of mitochondrial disease (Peter *et al.*,

2018; Nimmo *et al.*, 2019).
In our laboratory the use of NGS technology allowed us to identify three different mutations in *LONP1* gene in one patient showing a phenotype characterize by non-progressive ataxia and cerebellar atrophy. In my thesis I have functionally characterized the mutation in patients' fibroblast and used *S. Cerevisiae* as an *in vivo* model and an *in silico* structural model to evaluate the pathogenicity of these mutations.

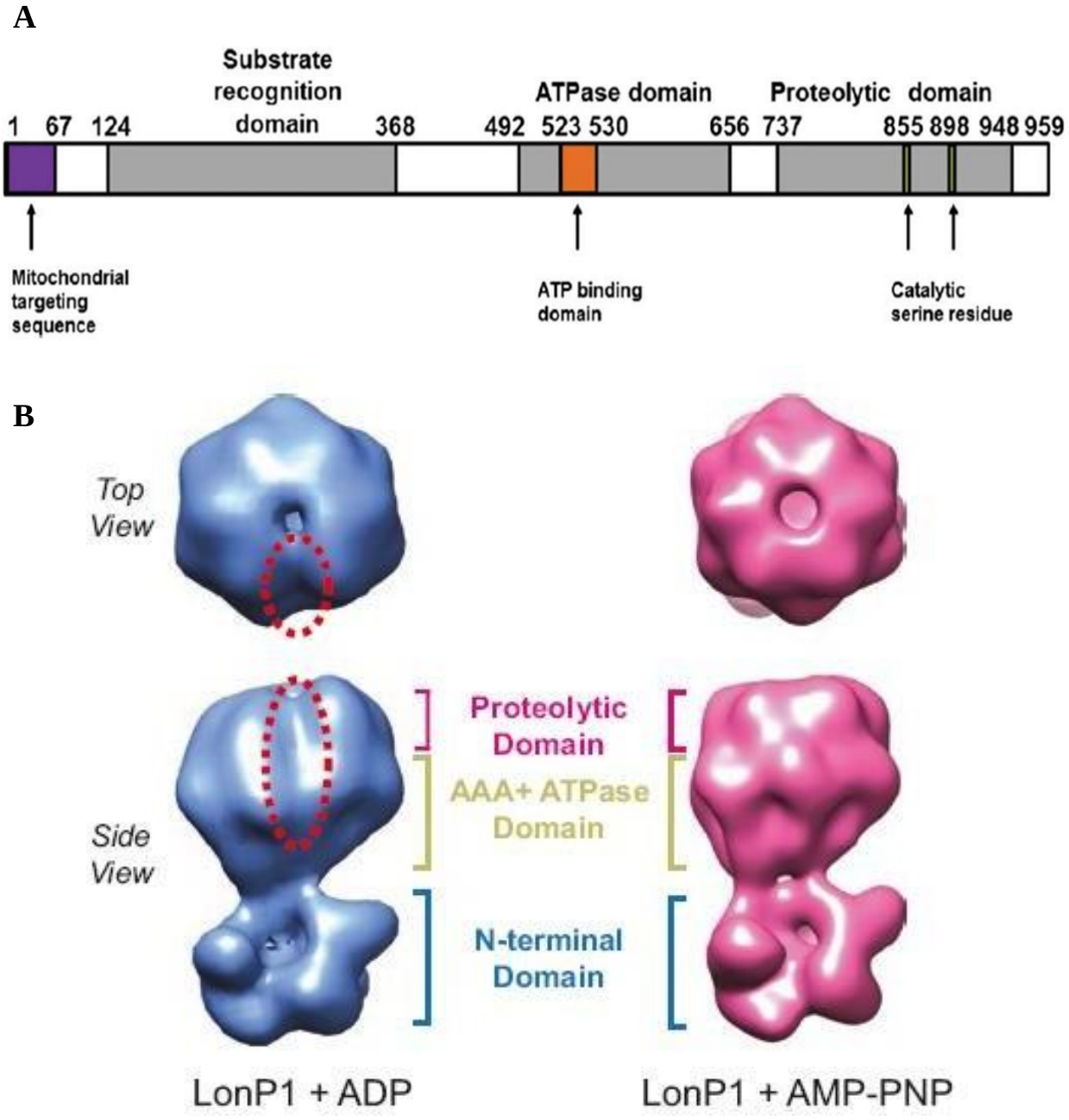

Figure 9: Lon domains and oligomeric structure. (A) Functional domains of Lon (Pomatto, Raynes and Davies, 2017) (B) Structure of human Lon oligomer (Wong and Houry 2019).

Results

Case report

The patient is a 17 years old female, born at term. She presents perinatal hypoxia due to dystocic delivery, psychomotor delay (walked at 2.5 years) and a normal language development. Furthermore, she presents a non-progressive ataxia, nystagmus and mild dysmetria and neuroimaging showed cerebellar atrophy (**Fig.10**). Only skin biopsy was performed in patient.

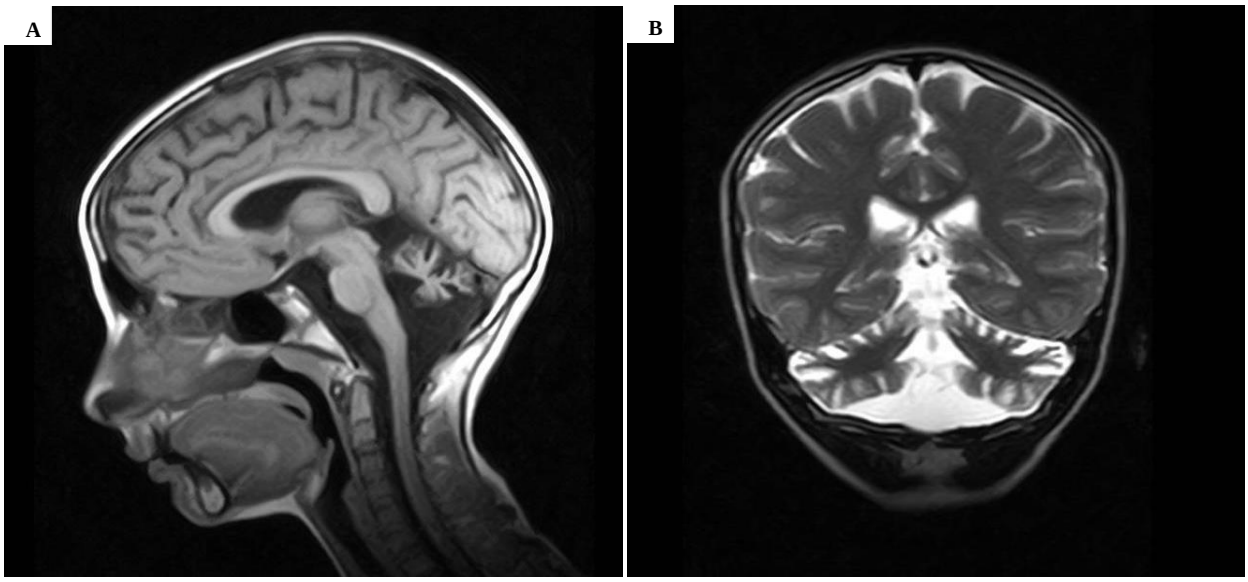

Figure 10: **Neuroimaging studies.** T1 weighted mid-sagittal section (a) and T2 weighted coronal section (b) of the mutated patient, showing global cerebellar atrophy without cortical or brainstem involvement

Mutational and structural analysis

We performed whole-exome sequencing (WES) on genomic DNA and, after excluding previously annotated single nucleotide changes occurring with high frequency in populations (>1%), we prioritized variants predicted to have functional impact by using *in silico* programs such as Sift, Poliphen2 and Human Splicing Finder [HSF]. Filtering analysis allowed us to identify three different candidate genes overlapping patients' phenotype: *NDUFS2*, *QARS* and *LONP1*. The first gene was excluded because we have found only one heterozygous mutation and is reported that mutations in this gene have a recessive inheritance. *QUARS* presented two intronic variants but the cDNA evaluation and the neuroimaging analysis lead us to exclude them. Finally, we found three heterozygous mutations in *LONP1* gene. Two of these mutations were missense, one located in exon 12 (c.1879C>T (p.Pro627Ser)) and the other located in exon

18 (c.2716G>T (p.Gly906Trp)); the third was an intron variant (c.429+4A>G). Mutations' segregation was confirmed using Sanger sequencing (**Fig.11**): the two missense mutations were inherited from the father, while the intron variant was inherited from the mother. Analysing the missense mutations using *in silico* pathogenic prediction tools (Sift, Poliphen2 and Human Splicing Finder [HSF]), we observed that the p.Pro627Ser is predicted as deleterious only in Sift but tolerated in Poliphen2; and the p.Gly906Trp was predicted as damaging in both programs. The intron mutation analyzed by HSF is predicted to produce an alteration of the WT donor site of intron 1, then affects the splicing. Both the missense variants are conserved in different species (**Fig.12A**)

To further analyze the effect of the two missense mutations at a protein level we used an *in silico* three-dimensional structural model. From this model (**Fig.12B**), it appears that Pro627, in the ATPase domain, may be replaced by a serine without perturbing the protein structure. Although, a proline to serine substitution usually lead to a loss of thermostability and also in our case, we hypothesize that this destabilization cannot compromise the protein function. On the contrary, there is no room to accommodate a bulky tryptophan at position 906 of the functional Lon structure without perturbing it. Therefore, replacement of Gly906, in the protease domain, with a bulky tryptophan would result in clashes with other residues, specifically with residues of the linker between the ATPase and protease domain (Val753 and Glu754), unless a significant conformational rearrangement occurs. Such a structural change could in principle impair a proper functionality of the mutant.

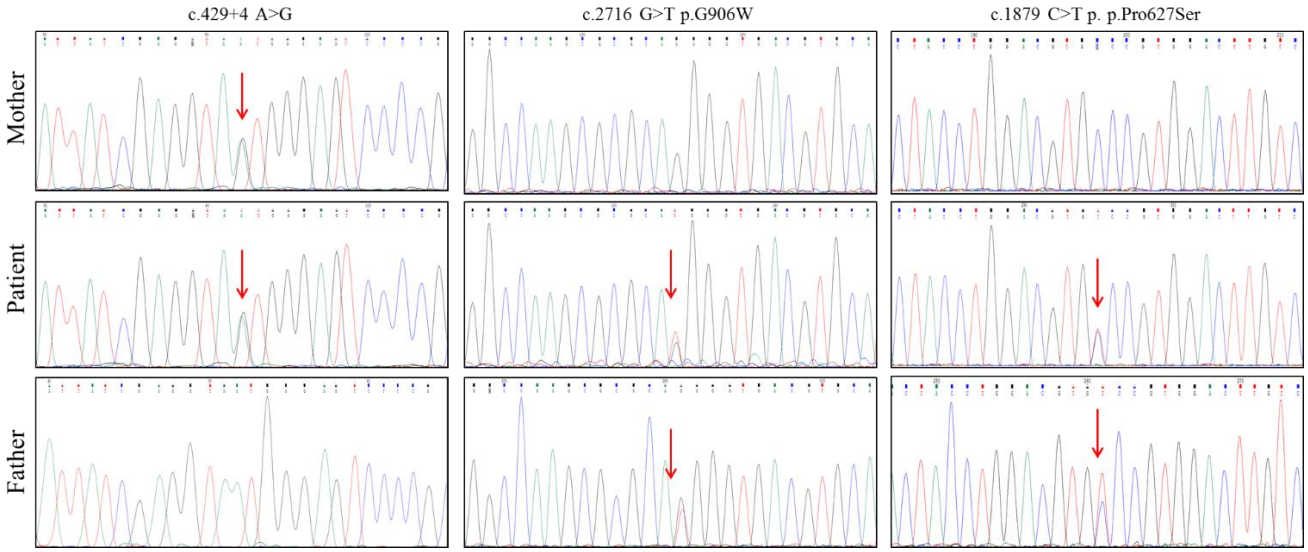

Figure 11: Electropherogram of patient and their parents. Validation of data obtained by WES and segregation of the different variants in the family.

A

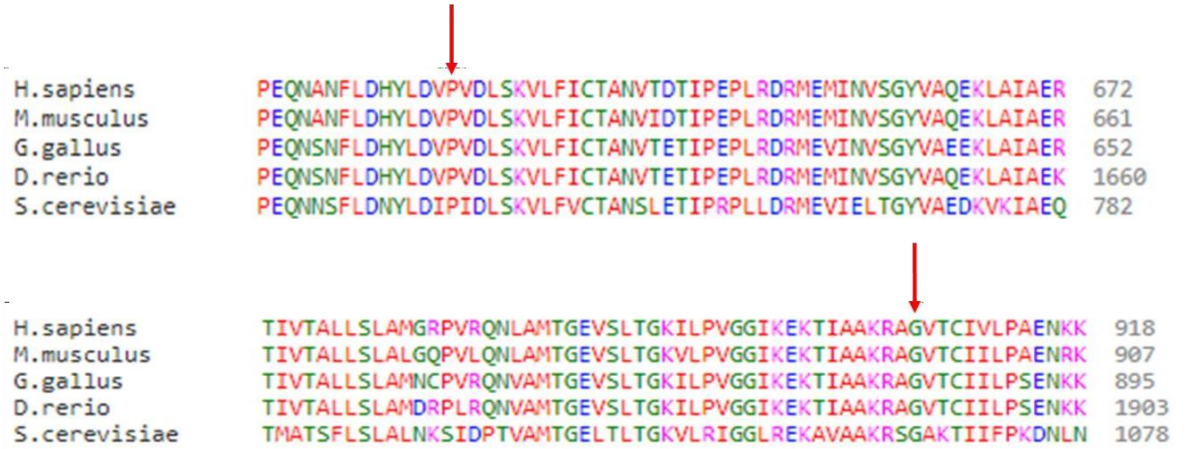

B

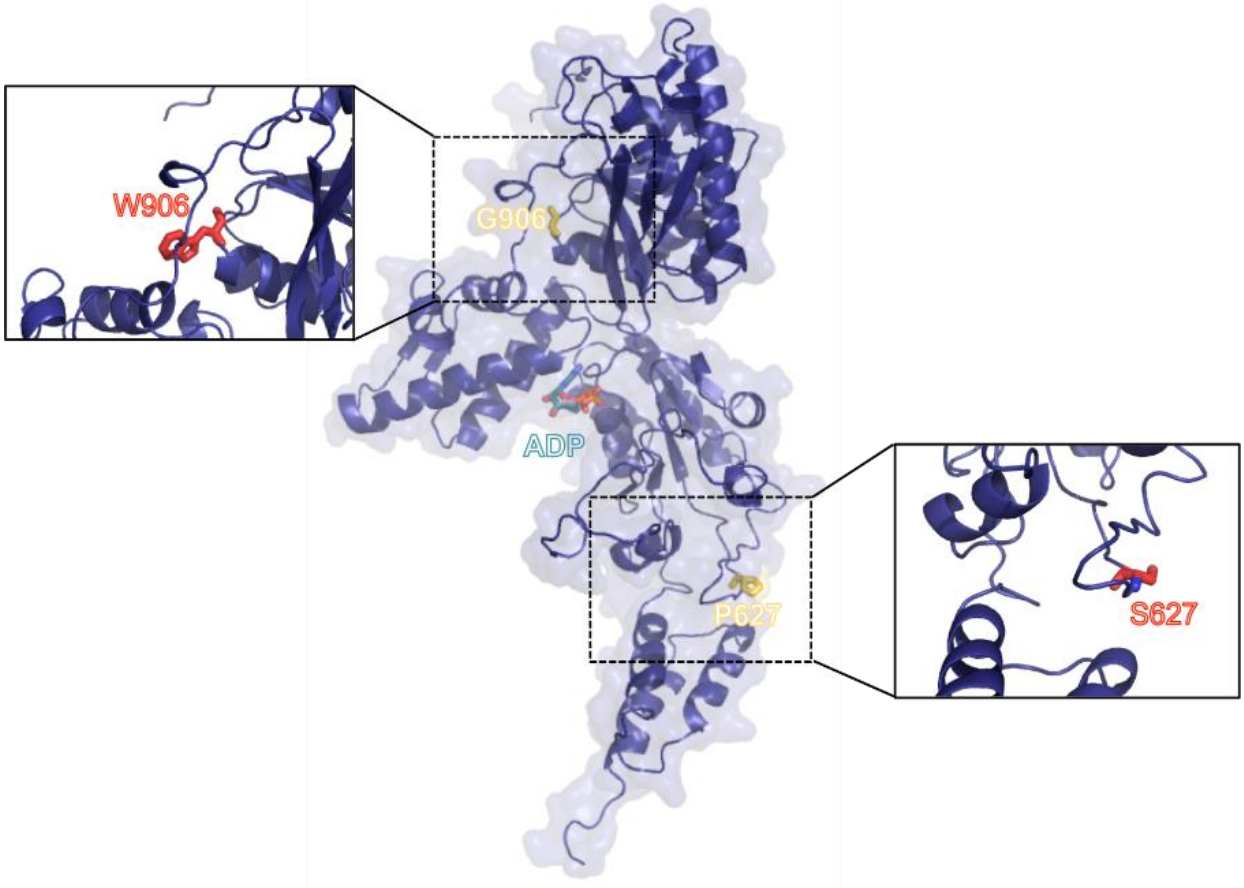

Figure 12: Conservation and 3D structural model. (A) Multiple sequence alignment among species. Arrows indicate the mutated aminoacidic residues (P627S and G906W). (B) Structural mapping of residues affected by the missense mutations.

Immunoblotting, biochemical and immunocytochemistry analysis

We performed Western blotting analysis in patient and controls fibroblast to evaluate the impact of the mutations on LONP1 stability and on the different subunits of the respiratory chain complexes (**Fig.13**). We observed a significative reduction of 50% of the protein Lon in patients compared to controls, and any variation in the OXPHOS subunits. Same results have been obtained using isolated mitochondria from fibroblast (data not shown). Although we have seen no reduction of the subunits of the respiratory chain complexes, therefore we decide to evaluate the rate of ATP synthesis in patients' fibroblast to assess the functionality of the mitochondria. The CV (ATP synthase) activity was measured in the direction of ATP synthesis using succinate (Succ), malate (Mal) or malate plus pyruvate (Mal+Pyr), as substrates. Results shows a reduced ATP synthesis with all substrates used (Succinate: -30%, Malate: -60% and Pyruvate + Malate: - 60%), pointing to multiple defects of the respiratory chain complexes (**Fig. 14**). We also analyzed the distribution of the Lon protein within the cell (**Fig.15**), which typically follows the mitochondrial network but, in the patient, we have observed a very lower intensity of the signal. These results confirm the reduction of the protein, already seen in the western blot analysis. Moreover, to analyzed the mitochondrial network we used an antibody against TOM20, in basal condition and in stress condition using galactose for 24 or 48 hours, to force the cell to produce ATP through the OXPHOS. As we can see in **Fig.16** the cells of the patient in basal condition show a mixed population with dot shaped, fixed and normal mitochondria; this different morphology of mitochondria is evident also in a single cell. When patients' fibroblasts were stressed with 24h of galactose treatment, cells show mitochondria very similar to the cell in basal condition with a mixed population but we can observe a remarkable trend to a fixed network more than the non-treated cells; after 48h of treatment the patients' fibroblasts shows a totally disorganized network with mitochondria all fixed.

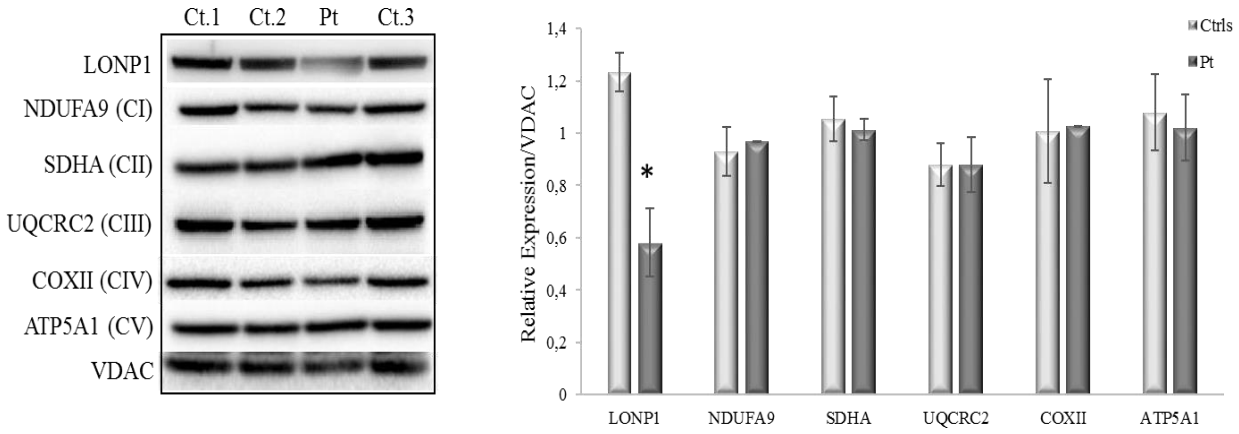

Figure 13: Western blotting analysis. Immunoblot of total lysates from control subjects (Ct) and patient's (Pt) fibroblasts using Lon, Ndufa9, SDHA, Uqcrc2, COXII, ATP5A1 and α-VDAC antibodies. The latter was used as loading control. Lon is 50% reduced and the OXPHOS subunits are normal compared to. Values in the graph are given as the mean ± SD (n = 3 to 4); *, p<0,05.

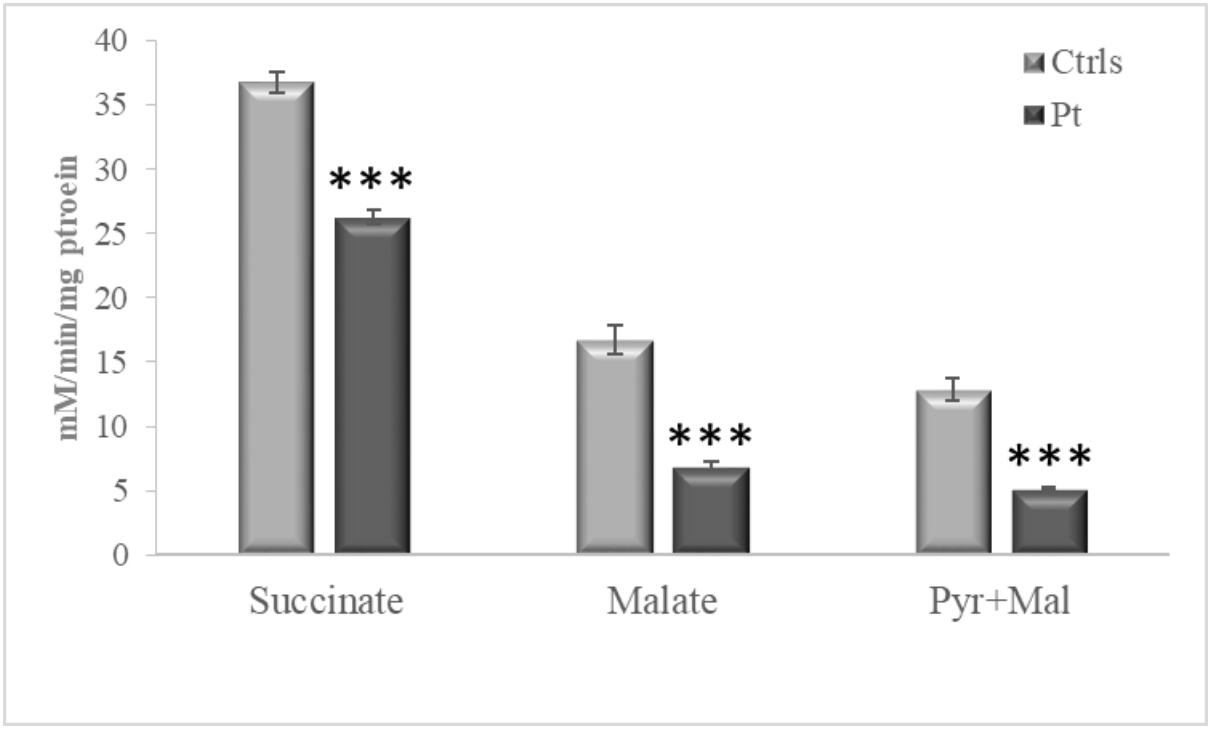

Figure 14: ATP synthesis. Patient show a reduction in ATP synthesis with Succinate, Malate and Pyruvate+Malate. Values in the graph are given as the mean ± SD (n = 3 to 4); ***, p<0,0005.

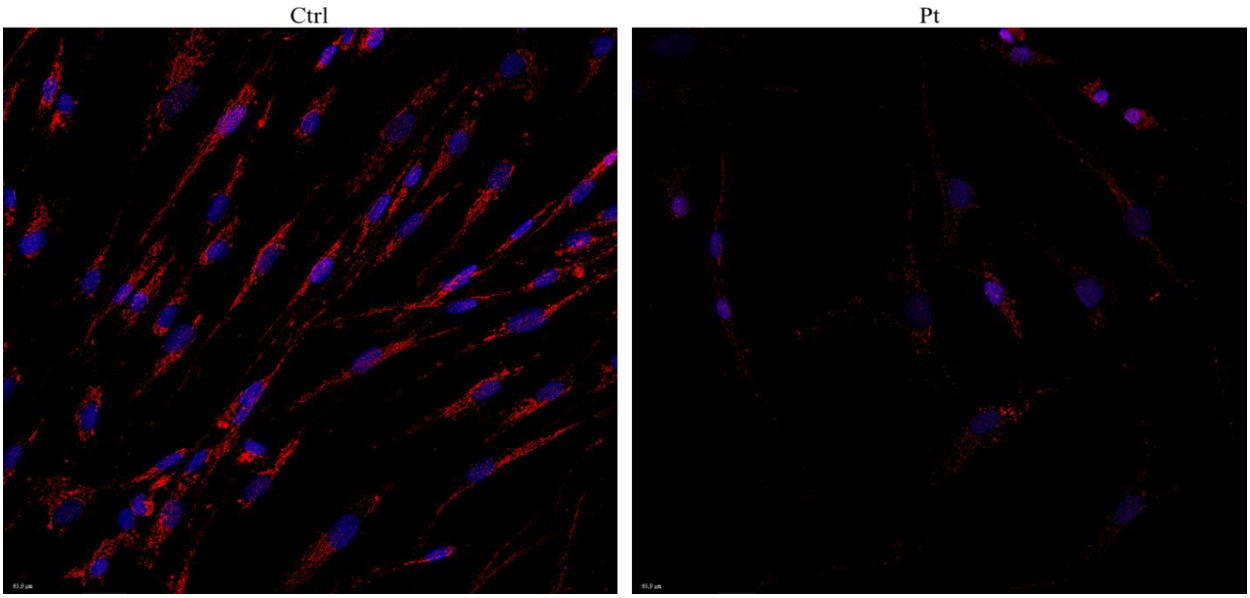

Figure 15: Immunocytochemistry analysis of Lon. Analysis of the protein's distribution in patients' and controls' fibroblast. Patient show a reduction in the signal.

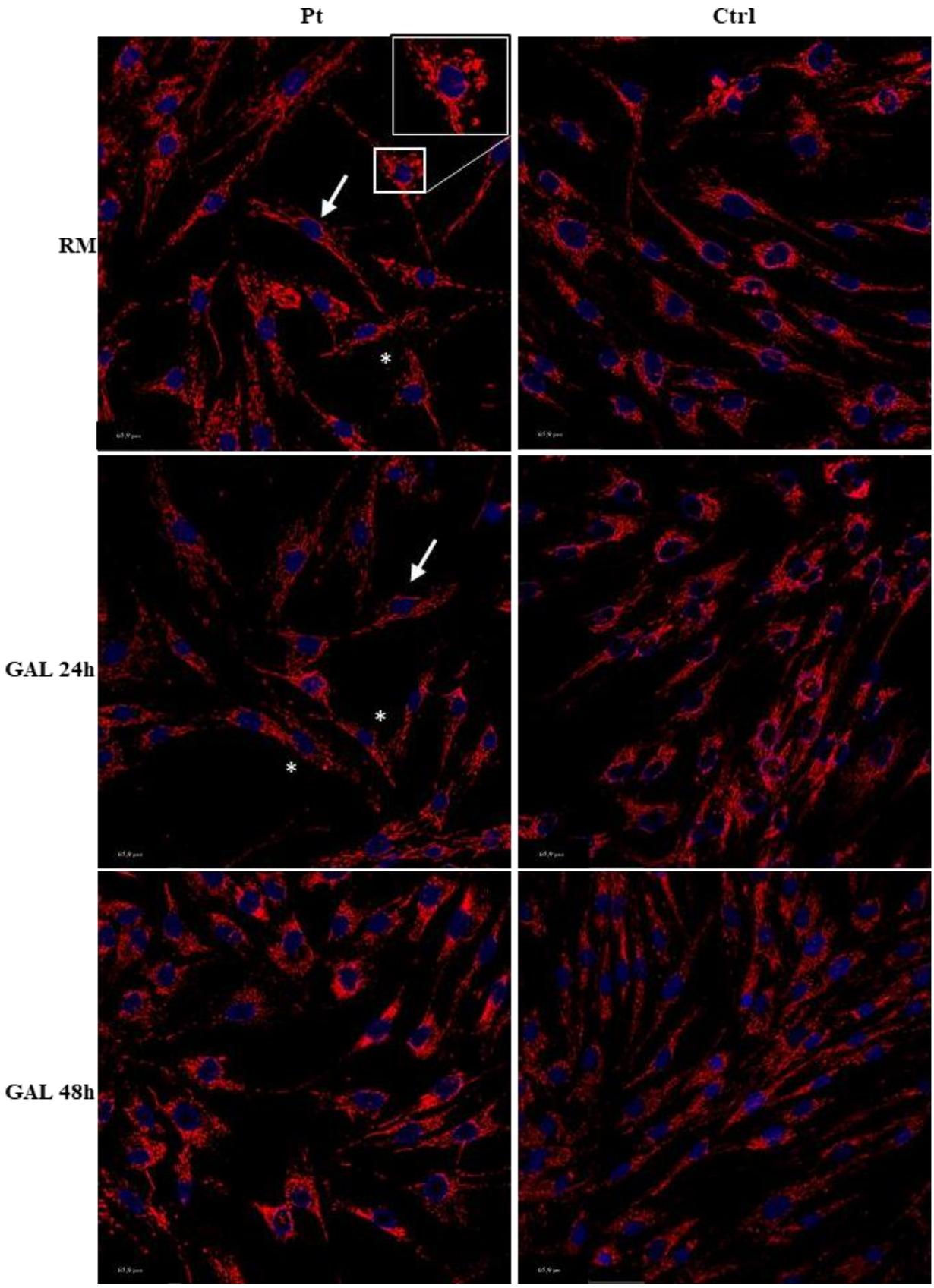

Figure 16: Immunocytochemistry mitochondrial network. Patient's and control's fibroblast cultured in regular medium or galactose medium (24h or 48h) and marked with TOM20 antibody. Arrows: cells with a normal mitochondrial network; Stars: cell with fixed mitochondria.

Yeast experiments

We used a yeast *Saccharomyces cerevisiae* as model to evaluate the pathogenicity of the mutation. *PIM1* is the yeast homologous of *LONP1* in human: the aminoacidic sequence is conserved between the two species with an identity of 44%. To further study this model we analyze the effect of the deletion of *PIM1* (*PIM1*Δ) in different growth conditions, The effect of the deletion of the *PIM1* gene on growth in fermentative or respiratory media in the deleted strain and in the wild type

(WT) strain has been compared (**Fig.17A**): the growth at the permissive temperature of 28°C of the deleted strain is slightly reduced in glucose but in glycerol medium is totally abolished. This demonstrates how *PIM1* is necessary for the respiration of the cell and that its deletion prevents a proper mitochondrial functionality. It is important to note that the *PIM1*Δ strain is thermo-sensible: at non-permissive temperature of 37°C the growth is totally prevented. The oxygen consumption capability of the *PIM1*Δ strain is also completely abolished (**Fig. 17B**).

Due to the role of *PIM1* in maintaining the integrity of mitochondrial genome, we evaluated the effect in mtDNA stability through a qRT-PCR experiment: we compared the level of mtDNA in the WT and in the *PIM1*Δ strain (**Fig 17C**). As expected, we observe a dramatic reduction of mtDNA copy number in the *PIM1*Δ strain compared to WT.

Finally, we evaluate the functionality of the mitochondrial membrane through DASPMI staining (**Fig 17D**): this stain can identify Δψ potential defects binding only to active membranes. The fluorescence microscopy images reveal a functional mitochondrial network in the WT strain; on the contrary the *PIM1*Δ strain shows collapsed, disorganized and dysfunctional mitochondrial network. The transformed WT and *PIM1*Δ cells expressing GFP in the mitochondria confirm the abnormal mitochondrial distribution as collapsed wide dots in the deleted strain (**Fig. 17E**).

To complement the *PIM1* deletion the endogenous gene has been reintroduced into the cells by plasmid transformation. Fig. **18A** shows the growth of serial dilutions of the WT, of the *PIM1*Δ mutant and of three clones transformed with the centromeric pC_PIM1 plasmid, in which the *PIM1* was cloned with its promoter. The reintroduction of the *PIM1* is not able to rescue the respiratory defect of the mutant in fact, the transformants do not grow in the respiratory medium. In fermentative medium the recovery of defects is observed, in particular at 28° C. By qRT-PCR the transcription level of the *PIM1* was analysed (Fig.

18B): in the three transformed clones the *PIM1* transcription level is higher compared to the WT (between 4000 and 100 times). It is possible to speculate that the lack of phenotypic recovery of the pC_PIM1 transformants may be due to the overexpression of PIM1 gene, which could be toxic for the cell. In fact, in clone 10 the *PIM1* transcription level is more similar to the WT and lower compared to the other two clones; in addition, also mitochondrial morphology of clone 10 is more similar to the WT (Fig. **18C**); suggesting that this transcript level of *PIM1* could be less toxic.
The complementation failure is also observed by qRT-PCR (Fig. **18D**): compared to the WT the transformants show a lower number of mtDNA copies.
By DASPMI staining it is possible to observe that the mitochondrial network of the transformants does not have an organized and defined structure: collapsed mitochondria are evident. Despite this, it is possible to note differences between clones 8 and 9, and clone 10: in some cells of the clone 10 the mitochondrial morphology is more similar to the physiological one, although many cells have collapsed mitochondria (Fig. **18C**). We can speculate that the complementation failure is maybe due to an impossibility of the transformants to recover the sever lack of mtDNA caused by *PIM* deletion. To obtain the complementation of the phenotype other experiments are on-going and our future perspectives is to further evaluate the pathogenicity of our patients' mutations with a mutagenic approach.

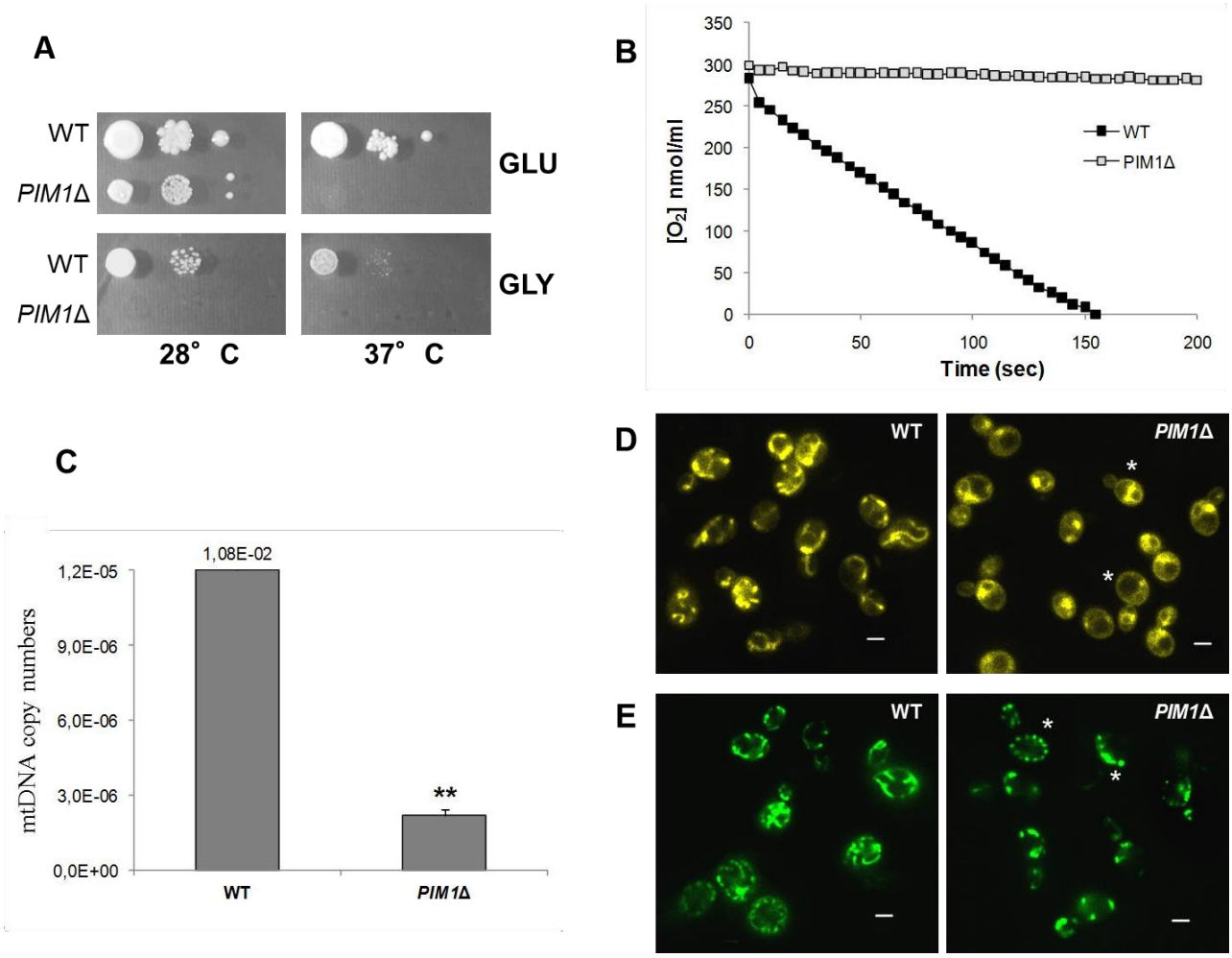

Figure 17 Phenotypic characterization of *PIM1*Δ yeast strain. (A) Serial dilutions of WT and WT deleted of PIM1 gene (*PIM1* Δ) were spotted on YP plates containing 2% glucose or 3% glycerol (upper and lower panels, respectively) as carbon source and incubated at 28 and 37 °C. (B) Oxygen consumption rate, expressed as O2 nmol/ml of WT (black), and its derivative *PIM1*Δ strain (white), grown in YP 2% glucose containing medium. (C) qRT-PCR analysis of mtDNA level of the WT and *PIM1*Δ strain, grown in YP 2% glucose containing medium. The ratio between nuclear DNA and mtDNA mean values (OXI1/ACT1) was used to overcome the variability among samples caused by total DNA quality. **P<0.01 for deleted versus WT strain, t Student test. (D-E) Fluorescence microscopy of mitochondrial tubular network stained with DASPMI of WT and *PIM1*Δ strains (D) or WT and *PIM1*Δ expressing GFP in the mitochondrial network (E). Strains were grown overnight in YP 2% glucose containing medium. Star indicate collapsed mitochondrial network. Scale bars: 2 μm.

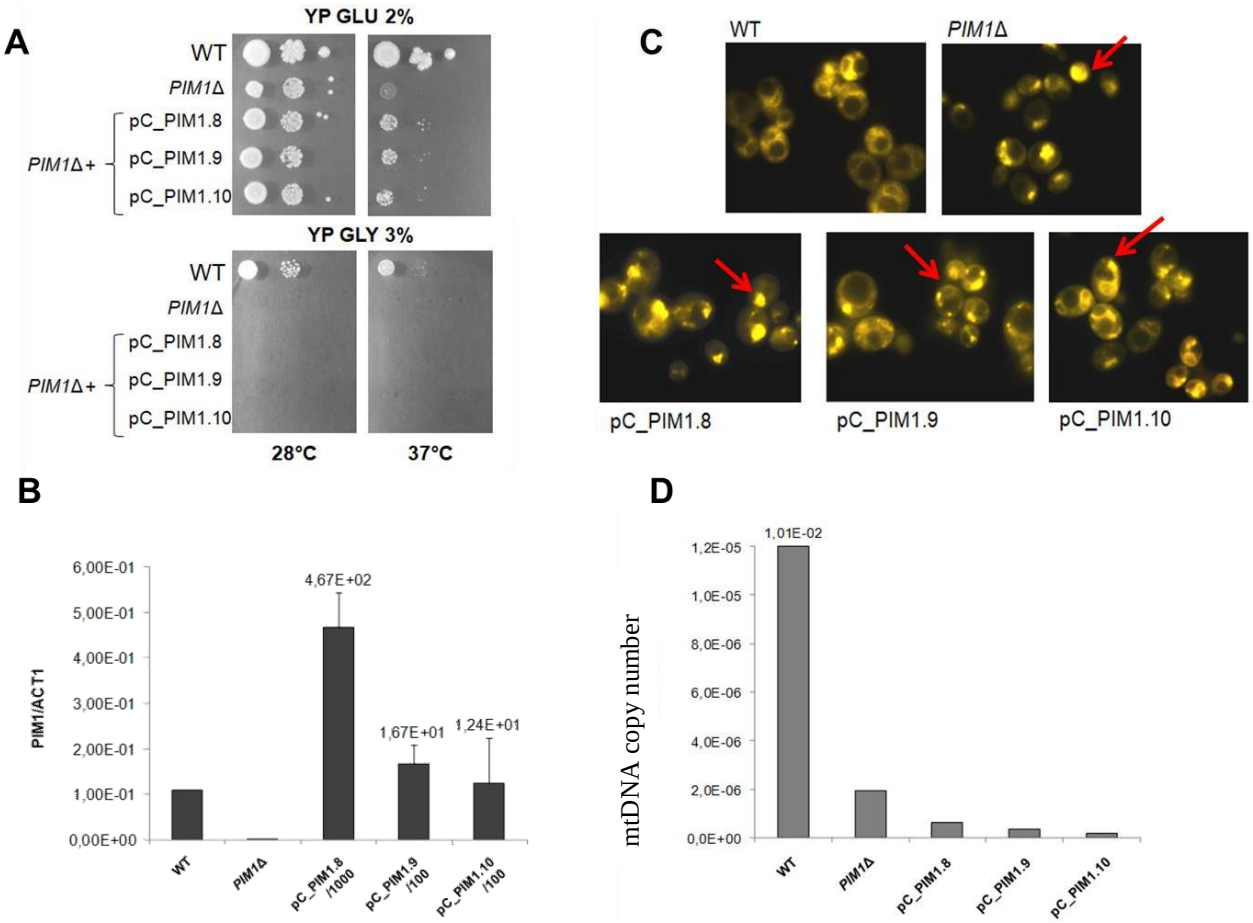

Figure 18 Complementation of mitochondrial defects (A) Spot of serial dilutions of the WT, *PIM1Δ* and three transformants clones (pC_PIM1.8, .9 and .10) strains on YP GLU 2% and YP GLY 3% containing media at 28° C (left images) and 37° C (images on the right). (B) Quantification by qRT-PCR of the *PIM1* transcript level of the same strains as above. Quantification is given by the ratio between the transcription level of the PIM1 gene and the housekeeping ACT1 gene. The value of the transformants has been divided by 1000 or by 100 to be displayed in the graph. (C) DASPMI staining of the mitochondrial network of the same strains as above. The red arrows show the representative mitochondrial morphology for each strain. (D) qRT-PCR analysis of mtDNA copy number of WT, *PIM1*Δ and transformed clones (PC_PIM1.8, .9 and .10). Quantification is given by the ratio between the copies number of the mitochondrial OXI1 and the nuclear ACT1.

Discussion

Lon is a multifunctional enzyme involved in different regulatory pathways inside the mitochondrial matrix. It was demonstrated that attempts to get a Lonp1-/-mice failed (Quiros *et al*. 2014), as Lon inactivation is lethal at embryonic stage, indicating the vital importance of this protein in mammals. In our laboratory, through NGS technology, we found three new mutations in *LONP1* gene in one patient with a clinical phenotype different from other described *LONP1* patients. Mutations in this gene cause a spectrum of clinical signs ranging from bilateral cataract to severe neurodegenerative diseases. It has been demonstrated that *LONP1* mutations can lead to a pathological condition known as CODAS (Cerebral Ocular Dental Auricular Skeletal) syndrome that, in addition, shows symptoms resembling a mitochondrial disease such as hypotonia and sensorineural hearing loss. To date, 12 missense mutations in *LONP1* are associated with CODAS syndrome, either homozygous or heterozygous and the majority fall into the ATPase domain (Strauss *et al*. 2018); other 10 missense mutations were associated with congenital cataract, all were homozygous , mapping in the ATPase domain too (Khan and AlBakri, 2018). In 2017 was reported a patient with two heterozygous variants, one in the N-terminal domain and one in the proteolytic domain; in this case the patient presented motor regression, involuntary movement and cerebellar atrophy without involvement of skeletal or dental symptoms; these features have never been reported in CODAS syndrome but are more indicative of a mitochondrial disease (Inui *et al.*, 2017). Finally, in 2018, Peter *et al*. reported compound heterozygous missense mutations in *LONP1*, both located in the ATPase domain, in a patient characterized by a classic mitochondrial phenotype, with Leigh syndrome, lactic acidosis, respiratory distress, reduced movement and a severe multiple OXPHOS defects. More recently, two siblings have been reported with a homozygous missense variant in the protease domain of *LONP1* associated with a severe neurodegenerative phenotype, presenting a progressive cerebral and cerebellar atrophy, developmental delay and, in one of the two siblings, seizures refractory too (Nimmo *et al.*, 2019).

The patient here described is characterized by psychomotor delay, non-progressive ataxia, nystagmus and severe cerebellar atrophy. Therefore, the clinical phenotype of our patient is milder than the one previously reported (Strauss *et al*. 2015; Peter *et al*, 2018; Nimmo *et al*.2019). In patient's fibroblasts, we observed that *LONP1* mutations cause defects in mitochondrial functionality and morphology. Moreover, the alterations of mitochondrial network are more

evident after galactose administration, indicating that Lon is fundamental to maintain mitochondrial homeostasis. Our results are in line with the previously reported electron microscopy imaging that showed abnormal mitochondria (Nimmo *et al*. 2019). In addition, western blot analysis revealed a 50% reduction of Lon, which can be due to the splicing mutation; this variant could produce an exon skipping that can lead to a decay of the mRNA and/or to a degradation of the protein.

We can speculate that the intronic variant, which affects the total amount of the protein, lead to a loss of function resulting in a less severe phenotype.

We are deeply investigating the missense mutations in the yeast model, in order to better characterize the variants' effect. In conclusion, the features of our patient expand the clinical phenotype caused by mutations in *LONP1*.

Methods

Standard protocol approvals, registrations and patients consents

The study was approved by the Ethical Committees of the Bambino Gesu` Children's Hospital, Rome, Italy, in agreement with the Declaration of Helsinki. Informed consent was signed by the parents of the patients.

Mutational analysis

Exome capture and massively parallel sequencing were outsourced (BGI, Shenzhen, China) using Sure Select Human All Exon V.4 Agilent and deep Illumina Hiseq technology (median reads depth= 50×). Called variants were filtered to retain variants with a quality score (Qs) > 30. High- quality variants were then filtered against public databases (dbSNP142 and ExAC v.0.3) to retain novel and clinically associated variants, and annotated variants with unknown frequency or having MAF< 1%. Variants prioritization was performed valuating their functional impact, using *in silico* programs for mutations (Sift, Poliphen2 and Human Splice Finder). All variants identified by NGS were validate by Sanger Sequencing as well the segregation in the family.

Structural model

A model for the ATPase and protease domains of LONP1 was built by Modeller using the coordinates of the experimental structure of its catalytic (C-terminal) domain, from Met756 to Glu953 (PDB ID: 3x36, resolution 2 Å), and the structure of Lon protease from *Bacillus subtilis* bound to ADP (PDB ID: 3m6a, resolution 3.4 Å, sharing with human LONP1 a sequence identity of 46%), as a template for the ATPase domain (residues Ala416-Arg755) and its orientation relatively to the protease domain. Models for the P627S and G906W point mutants were obtained with the mutagenesis tool of PyMol, starting from the coordinates of the wild-type

model.

Immunoblotting and Immunostaining

Human fibroblasts were obtained from a diagnostic skin biopsy and grown in DMEM medium supplemented with 10% fetal bovine serum, 4.5 g/L glucose, and 50 μg/mL uridine.

For SDS-PAGE, 40 μg of fibroblasts homogenate were loaded in a 12% denaturating gel. Western blot (WB) was achieved by transferring proteins onto polyvinylidene difluoride (PVDF) membrane and probed with specific antibodies. Specific bands were detected using Lite A blot Extend Long Lasting Chemiluminescent Substrate (Euroclone, Pero (Mi), Italy). Densitometry analysis was performed using Quantity One software (BioRad, Hercules, CA, USA). RCC subunits were detected using the following monoclonal antibodies purchased from MitoScience (Eugene, OR, USA): Complex I – NDUFA9; complex II – SDHA; complex-III - UQCRC2; complex IV – COXII; Complex V – ATP5A1; porin (VDAC). anti-LONP1 (Novus Bio) 1:500 was also used.

To display the mitochondrial network arrangement, fibroblasts from Patient were fixed and permeabilized using methanol:acetone (2:1) for 10 min at room temperature, then a blocking solution containing 5% BSA in PBS was used. The polyclonal rabbit TOMM20 antibody (Santa Cruz Biotechnology) was applied overnight and visualized using Alexa Fluor 647 secondary antibody (Jackson Immuno Research), both antibodies were used at the dilution of 1:500. Images were acquired with a fluorescence inverted microscope (Leica DMi8). An average of 8 image planes was obtained along the z-axis at 0.2 μm increments using LASX 3.0.4 (Leica) software.

To display the LONP1 network cells were fixed in paraformaldehyde (PFA) 4% for 10’ at room temperature (RT) and permeabilized in triton 0.1% + FBS 5% diluted in phosphate buffer saline (PBS) for 20’. After blocking in bovine serum albumin (BSA) 5% for 1h at RT, a primary antibody anti-LONP1 (Novus Bio) 1:100 + NGS 1% in PBS were added overnight at 4°C. After three wash in PBS 5’ an Alexa Fluor 647 secondary antibody (Jackson ImmunoResearch) 1:500 + NGS 3% in PBS for 1h at 37° was applied. After three wash in PBS 5’ nucleous were stained with Hoechst- 33342 1:10000 for 5’ and then the coverslip was mounted in PBS/Glicerol 1:1. Images were acquired with a fluorescence-inverted microscope (Leica DMi8). An average of 8 image planes was obtained along the z-axis at 0.2 μm increments using LASX 3.0.4 (Leica) software.

ATP synthesis

ATP synthesis was assayed spectrophotometrically. In brief, about 300 μg

mitochondrial proteins were incubated in 20 mM Tris–HCl, pH 7.5, 150 mM sucrose, 1 mM ADP, 20 mM phosphate, 5 mM $MgCl_2$, 100 μM di-adenosine pentaphosphate, 10 mM glucose, 30 U of hexokinase, and one of the following: 50 mM succinate, 6 mM malate, 6 mM α-ketoglutarate or 12 mM/1.2 mM pyruvate/malate, at 37°C for 20 min in vials with vigorous stirring to ensure maximum oxygenation. The reaction was stopped with 25 mM EDTA + 2 μM carbonyl cyanide 3- chlorophenylhydrazone (CCCP), followed by transfer to ice-cold water. The synthesized glucose 6-phosphate was oxidized by NADP in the presence of 30 units of glucose 6-phosphate dehydrogenase. NADPH formation was monitored at 340 nm. Under these experimental conditions, a 1:1 ratio was found between the ATP synthesized and the NADPH formed. Protein content was measured by BCA (Pierce, USA) and read at 562 nm.

Yeast experiments

Yeast strains used to perform experiments described in this thesis were the D273–10B/A1 (MATα, met6, ura3-52; Sherman e Slonimski, 1964) rho+ (with mtDNA wild type). The *PIM1* null strain (*PIM1*Δ) was obtained by transformation of D273–10B/A1 (MATα, met6, ura3-52) rho+ with the Kan-MX4 cassette as already described (Montanari *et al.*, 2013).

Strains were grown on YP complete medium (1% yeast extract and 1% peptone from Difco) containing, 2% glucose or 3% glycerol or in minimal medium (0.17% yeast nitrogen base -Difco, 0.5% ammonium sulfate and 2% glucose), supplemented with the necessary auxotrophic requirements according to the phenotype of the strains. For plates, 2% agar was added to the medium. Growth capability was investigated by serial dilutions from concentrated suspensions (5×10^6 cell/ml) prepared from fresh single colony spotted onto YP agar plates containing 3% glycerol or 2% glucose. Pictures were acquired after 2–3 days of growth on glucose plates and after 5 days of growth on glycerol plates.

Transformation of yeast strains was obtained by the lithium acetate method (Gietz and Woods, 2014). To control *PIM1* deletion, colony PCR has been performed. Cells were resuspended in 100 μl of LiAc 0.2 M + SDS 1%. After incubation at 70° C for 15 min, 300 μl of EtOH were added. After vortexing and centrifugation at 13,000 rpm for 3 min, the supernatant was removed and the pellet was resuspended in 100 μl of TE 1X. Vortex again and centrifuge at 1,000 rpm for 1 min. PCR protocol using 3PIM1+ / KANRev primers was as follow: 5’ at 95°C; 40 X (30 sec at 95°C;, 40 sec at 60 °C, 1 min at 72°C); 1 min at 72°C .

Standard protocols (Sambrook et al, 1989) were used for restriction enzyme digestions as well as plasmid preparations.

To produce pC_PIM1 plasmid, PCR amplification using 3'PIM1+ and 5'PIM1- was performed to clone PIM1 gene with its promoter in the commercial pCR2.1TOPO plasmid (Invitrogen). The insert was successively subcloned in the centromeric pRS416 plasmid by *KpnI*/*XhoI* digestion.

Respiration studies were performed using a Clark oxygen electrode (Hansatech Instruments). After overnight growth in YP 2% glucose containing medium at 28°C cells were washed with 1 ml sterile water. After centrifugation the pellet, corresponding approximately to 0.03 g (wet weight) of cells, was suspended in 1 ml of phosphate buffer10 mM, pH 7.4 containing 0.4% glucose and loaded in the Reaction Vessel of the previously calibrated Oxygen Electrode Chamber. The endogenous oxygen consumption was measured for 10 min.

To quantify the numbers of mtDNA copies we performed a quantitative Real Time-PCR (qRT- PCR) assay using 2X SYBR-green master mix (Bioline) and primers for the mitochondrial OXI1 gene and ACT1 gene as a housekeeping gene. For RT-PCR experiments the total RNA extraction, cDNA generation, sample preparation and amplification reaction were performed as previously described (Montanari, Francisci 2017).

For detection of mitochondrial morphology yeast cells were transformed with multi-copy plasmid, pVT100U bearing the GFP gene with the mitochondrial presequence of ATPase subunit 9 of *Neurospora crassa* fused at 5'-end (Westermann and Neupert, 2000). To visualize mitochondrial functionality, we used DASPMI [2-(4-(dimethylamino)steryl)-1-methylpyridinium iodide], a vital staining that reveals mitochondrial functional membranes. Image were acquired in the Zeiss Axio Imager Z1 Fluorescence Microscope and elaborated through an Axio-Vision 4.8 Digital Image Processing System and objective lens 63× oil.

Oligonucleotides:

PIM1Kan+	5’-GGTTTTCGAGGTGCTTGAACGAAAAGATTTGCAAATAGAGCGTACGCTGCAGGTCGAC-3’
PIM1Kan-	5’-CAGAATGTTTAAACAGGTATTTAATCCATTTAGATGAAAAGTTCGACACTGGATGGCGGC-3’
3’PIM1+	5’-TCTTCGGTAAGTAATTAGATTTC-3’
5’PIM1+	5’-GTAGATCGCAAAAGTTGCTAG-3’
KANRev	5’-TCATGCCCCTGAGCTGCG-3’
PIM1.2+	5’-TGACAGAAGATGCAATAACAG-3’
PIM1.2-	5’-CTTTCTTTAGGCTTGCTGTC-3’
ACT1+	5'-ACGTTCCAGCCTTCTACGTTTCCA-3'
ACT1-	5'-AGTCAGTCAAATCTCTACCGGCCA-3'
OXI1+	5'-GTACCAACACCTTATGCAT-3'
OXI1-	5'-CATTCAAGATACTAAACCTAA-3'

References

Francisci, S., Montanari, A., (2017) 'Mitochondrial diseases: Yeast as a model for the study of suppressors', BBA-Molecular Cell Research 1864, 666-673.

Fu, G.K., Smith, M.J., & Markovitz, D.M. (1997). Bacterial protease Lon is a site-specific DNA-binding protein. Journal of Biological Chemistry, 272(1), 534-538.

Fu, G. K., & Markovitz, D. M. (1998). The human LON protease binds to mitochondrial promoters in a single-stranded, site-specific, strand-specific manner. Biochemistry, 37(7), 1905-1909.

Gietz, R. D. and Woods, R. A. (2014) 'SpringerProtocols: Abstract: Yeast Transformation by the LiAc/SS Carrier DNA/PEG Method', Yeast Genetics, 313(4).

Inui, T. et al. (2017) 'A novel mutation in the proteolytic domain of LONP1 causes atypical CODAS syndrome', Journal of Human Genetics, 62(6), pp. 653–655.

Khan, A. O. and AlBakri, A. (2018) 'Clinical features of LONP1-related infantile cataract', Journal of AAPOS. Mosby Inc., 22(3), pp. 229–231.

Lu, B. et al. (2007) 'Roles for the human ATP-dependent Lon protease in mitochondrial DNA maintenance', Journal of Biological Chemistry, 282(24), pp. 17363–17374.

Luce, K. and Osiewacz, H. D. (2012) 'Erratum: Increasing organismal healthspan by enhancing mitochondrial protein quality control (Nature Cell Biology (2009) 11 (852-858))', Nature Cell Biology, p. 220.

Luciakova, K. et al. (1999) 'Enhanced mitochondrial biogenesis is associated with increased expression of the mitochondrial ATP-dependent Lon protease', FEBS Letters.

Montanari, A. et al. (2013) 'Analyzing the suppression of respiratory defects in the yeast model of human mitochondrial tRNA diseases', Gene, pp. 1–9.

Nimmo, G. A., Venkatesh, S., Pandey, A. K., Marshall, C. R., Hazrati, L. N., Blaser, S., ... & Suzuki, C. K. (2019). Bi-allelic mutations of LONP1 encoding the mitochondrial LonP1 protease cause pyruvate dehydrogenase deficiency and profound neurodegeneration with progressive cerebellar atrophy. Human molecular genetics, 28(2), 290-306.

Peter, B. et al. (2018) 'Defective mitochondrial protease LonP1 can cause classical mitochondrial disease', Human Molecular Genetics, 27(10), pp. 1743–1753.

Pomatto, L. C. D., Raynes, R. and Davies, K. J. A. (2017) 'The peroxisomal lon protease LonP2 in aging and disease: Functions and comparisons with mitochondrial Lon protease LonP1', Biological Reviews, 92(2), pp. 739–753.

Quiros, P.M., Espanol, Y., Acin-Perez, R., Rodriguez, F., Barcena, C., Watanabe, K., Calvo, E., Loureiro, M., Fernandez- Garcia, M.S., Fueyo, A., et al. (2014). 'ATP-dependent Lon protease controls tumor bioenergetics by reprogramming mitochondrial activity'. Cell Rep. 8, 542–556.

Rep, M. et al. (1996) 'Promotion of mitochondrial membrane complex assembly by a proteolytically inactive yeast Lon', Science.

Sambrook, J., Fritsch, E.F., Maniatis, T., 1989. 'Molecular cloning: a laboratory manual.' ColdSpring Harbor Laboratory Press, Cold Spring Harbor, NY

Shebib, S. M. et al. (1991) 'Newly recognized syndrome of cerebral, ocular, dental, auricular, skeletal anomalies: CODAS syndrome - A case report', American Journal of Medical Genetics.

Strauss, K. A. et al. (2015) 'CODAS syndrome is associated with mutations of LONP1, encoding mitochondrial AAA+ lon protease', American Journal of Human Genetics. The American Society of Human Genetics, 96(1), pp. 121–135.

Wong K.S., Houry W.A. (2019) 'Recent Advances in Targeting Human Mitochondrial AAA+ Proteases to Develop Novel Cancer Therapeutics.' In: Urbani A., Babu M. (eds) Mitochondria in Health and in Sickness. Advances in Experimental Medicine and Biology, vol 1158. Springer, Singapore.

Westermann, B., Neupert, W., (2000) ‘Mitochondria-targeted green fluorescent proteins: convenient tools for the study of organelle biogenesis in Saccharomyces cerevisiae’, Yeast 16, 1421–1427

General conclusions and future perspective:

In my project I analyzed different patient presenting with different subtype of mitochondrial diseases; the use of Next Generation Sequencing technology, in the last years, has expanded the genetic diagnosis of many unsolved cases with mitochondrial disorders, with an increased diagnostic success, from <20% to >60% (Gorman *et al.*, 2016).

In my project I analyzed two different pathways involved in mitochondrial homeostasis. These pathways can actually underpin two mechanisms known as mitochondrial dynamics and quality control; both the proteins are involved in maintaining mitochondrial health and functionality. In particular, Drp1 is the main responsible of mitochondrial fission, a fundamental process during development; in fact, it drives a correct distribution of mitochondria during cellular division. On the other hand, Lon is a multifunctional protease involved in mitochondrial quality control and that take part to different mechanism such as mitochondrial and cellular proteostasis, mitochondrial DNA stability and folding of some of the subunits of the respiratory chain complexes (e.g. COXI, COXIV). Both, the murine model of *DNM1L* and *LONP1* homozygous knockout results to be embryonically lethal, underling the fundamental role of these two proteins in the whole physiology of mammals.

In the first part of my thesis I have characterize five patients with different mutations in *DNM1L* gene and, using different approaches, I have demonstrated that all mutations are pathogenetic; Next Generation sequencing technology was an useful tool, not only to identified the new different variant, but also to deeply investigate the variant of the patient 4, allowing us to demonstrate that was a germinal mosaicism of the mother, otherwise we had lack this information. It is important to note that we had demonstrated for the first time a particular feature of the muscular biopsy of patient mutated in *DNM1L* and that can be useful in the future to accelerate the diagnosis of patients presenting such phenotypic signs.

In the second part of my thesis I have characterized one patient with three different mutation in *LONP1* gene; this gene was already reported as the cause of very different pathology conditions such as CODAS syndrome or other type of disease that resemble a more classical mitochondrial disease. We here describe a patient with a milder phenotype in respect to the already referred patients. As already reported, we believe that different pathogenic Lonp1 variants may confers specific defect in protein degradation and can lead to different organ-specific dysfunction. Since there are no effective curative treatments in mitochondrial diseases, the individuation of disease-associated variants is of key importance and can lead us

to study, in the near future, specific therapeutic approaches that can modulate the functionality of these mutated proteins.

Synopsis

Mitochondria are subcellular organelles found in all eukaryotic cells, except in red blood cells; they are implicated in multiple cellular processes and consist of two membranes, the inner mitochondrial membrane (IMM) and the outer mitochondrial membrane (OMM), and of two aqueous compartments, the matrix and the intermembrane space. The IMM area is several-fold larger than the one of OMM, due to the fact that in the IMM there are some invaginations called *cristae* which contain the electron transport chain complexes from I to IV (complex I, CI; complex II, CII; complex III, CIII; complex IV, CIV) and the F1-F0-ATP synthase (CV). This multicomplex system is responsible for energy production, in the form of adenosine 5′-triphosphate (ATP), via the oxidative phosphorylation (OXPHOS).

In addition to energy production, mitochondria are involved in many biological functions, including the regulation of reactive oxygen species (ROS), biogenesis of the Fe-Cu clusters, heme synthesis, metabolism of amino acids and lipids, apoptosis and mitophagy (Gorman *et al*. 2016). Given their fundamental role in the physiology of the whole cell, mitochondria undergo to a tightly regulation, since any of their dysfunction can lead to dramatic consequences

Mitochondrial diseases (MDs) are a group of very heterogeneous and rare genetic disorders that affect mitochondrial respiratory chain function and cellular energy production. MDs can arise from both nuclear or mtDNA mutations, can occur at any age and, although the most affected tissues are those with high energy demand such as brain, muscle and heart, the clinical signs could involve also liver, heart, kidney, eye and ear (ref). The incidence of MDs is 1:5000 live birth (Gorman *et al*., 2016; Craven *et al*., 2017) considering only the mutation that affect the mtDNA and even higher by including some frequent nuclear gene mutations, reaching the incidence of 1:2000 individuals (Suomalainen and Battersby, 2018). In the last years, the breakthrough of next-generation sequencing (NGS) approaches for genetic diagnosis has expanded the genetic heterogeneity of MDs (Stenton and Prokisch, 2018).

The maintenance of "healthy" and fully functional mitochondria is essential for cellular homeostasis. In this regard, the cell has evolved various mechanisms dedicated to the maintenance of the mitochondrial proteome such as mitochondrial dynamics and mitochondrial quality control. A first check point and active surveillance is provided by the organelle itself. The mitochondria have their own chaperones and proteolytic enzymes that remove damaged or unfolded proteins (Matsushima and Kaguni, 2012). The plasticity of the mitochondria

allows continuous changes of their shape and number, while their morphology is maintained by the equilibrium of fusion and fission event.
Mitochondria undergo fusion and fission in order to avoid damage accumulation or respond to certain bioenergetics demands (Campello and Scorrano, 2010). In recent years, a significant number of mutations in genes involved in mitochondrial dynamics and mitochondrial quality control have been recognized as the genetic cause of MDs.
In our laboratory through the use of Next Generation Sequencing (NGS) technology we identify new mutations in genes involved in mitochondrial dynamics and in mitochondria quality control and we have functionally characterized these mutations and demonstrated their pathogenic roles in the analyzed patients.
In the first part of my thesis I focused my attention in the pathway of mitochondrial dynamics; this mechanism is controlled by a set of dynamin's family members, the large guanosines triphosphate hydrolases (GTPases) that are well conserved between yeast, flies, and mammals. Fission is mediated by a cytosolic dynamin family member called Drp1, encoded by *DNM1L* gene. When activated DRP1 is recruited by the mitochondrial dynamics' proteins 49 and 51 kDa (MiD49 and MiD51), and the mitochondrial fission factor (Mff) to the outer mitochondrial membrane, where it binds its receptor, the mitochondrial fission protein 1 (Fis1) and multimerizes, creating a ring-like structure that constricts and divides the organelle five patients presenting with epileptic encephalopathy The use of NGS technology allowed us to described five patients with different missense mutations in *DNM1L* gene and, using different approaches, I have demonstrated that all mutations are pathogenetic. Probably the most peculiar finding in the cohort of our patients is the muscle histology/histochemistry showing core like areas using oxidative enzyme staining for COX and SDH, which suggest an abnormal distribution of mitochondria in the muscle tissue. We found this pattern in all the examined muscle biopsies. Moreover, in serial sections of muscle fibers of Pt.3 we demonstrated that the fibers that are no reactive for COX, SDH and NADH are also negative for the staining with ATPase 9.4 indicating that these are type I muscular fibers.
In the second part of my thesis I study another pathway called mitochondrial quality control that is a mechanism involved in the maintenance of mitochondrial health and function. A set of chaperones and proteases, belonging to the AAA+-proteases (**A**TPases **A**ssociated with diverse cellular **A**ctivities) family, located in different mitochondrial compartment controls the biosynthesis, folding or

degradation of misfolded proteins. Lon, in the mitochondrial matrix, acts mainly as a protease but also as a chaperone to guide the folding of several respiratory chain complexes subunits (Rep *et al.*, 1996). Moreover, it can regulate the stability of the mtDNA, directly binding it (Fu, Smith & Markovitz, 1997) or indirectly regulating the degradation of the main transcription factor of the mtDNA, TFAM (Lu *et al.*, 2007). *LONP1* mutations have been associated to a severe disease, known as CODAS (Cerebral, Ocular, Dental, Auricular, Skeletal anomalies) (Shebib *et al.*, 1991; Strauss *et al.*, 2015) (OMIM #600373). Only recently *LONP1* mutations have been recognized as the genetic cause of a subtype of mitochondrial disease (Peter *et al.*, 2018; Nimmo *et al.*, 2019).

In our laboratory through the use of NGS technology I identify three different mutations in *LONP1* gene in one patient showing a phenotype characterize by non-progressive ataxia and cerebellar atrophy. In my thesis I have functionally characterized the mutation in patients' fibroblast and used *S. Cerevisiae* as an *in vivo* model and an *in silico* structural model to evaluate the pathogenicity of these mutations. In patient's fibroblasts, we observed that *LONP1* mutations cause defects in mitochondrial functionality and morphology. Moreover, the alterations of mitochondrial network are more evident after galactose administration, indicating that Lon is fundamental to maintain mitochondrial homeostasis. We are now deeply investigating the missense mutations in the yeast model, in order to better characterize the variants' effect. In conclusion, the features of our patient expand the clinical phenotype caused by mutations in *LONP1*.

In conclusion the use of NGS technology, in the last years, has expanded the genetic diagnosis of many unsolved cases with mitochondrial disorders and, since there are no effective curative treatments in mitochondrial diseases, the individuation of disease-associated variants is of key importance and a basic understanding of the molecular mechanism involved in these mitochondrial pathways can lead us to study, in the near future, specific therapeutic approaches that can modulate the functionality of these mutated proteins.

PUBBLICATIONS:

Verrigni D, Di Nottia M, Ardissone A, Baruffini E, Nasca A, Legati A, Bellacchio E, Fagiolari G, Martinelli D, Fusco L, Battaglia D, **Trani G**, Versienti G, Marchet S, Torraco A, Rizza T, Verardo M, D'Amico A, Diodato D, Moroni I, Lamperti C, Petrini S, Moggio M, Goffrini P, Ghezzi D, Carrozzo R, Bertini E. Clinical-genetic features and peculiar muscle histopathology in infantile DNM1L-related mitochondrial epileptic encephalopathy. Hum Mutat. 2019 May;40(5):601-618.